

8-2007

AN IN VITRO EVALUATION OF DBM AS A TISSUE ENGINEERED SCAFFOLD

Stephanie Arnold

Clemson University, slarnold@gmail.com

Follow this and additional works at: https://tigerprints.clemson.edu/all_theses

 Part of the [Biomedical Engineering and Bioengineering Commons](#)

Recommended Citation

Arnold, Stephanie, "AN IN VITRO EVALUATION OF DBM AS A TISSUE ENGINEERED SCAFFOLD" (2007). *All Theses*. 174.
https://tigerprints.clemson.edu/all_theses/174

This Thesis is brought to you for free and open access by the Theses at TigerPrints. It has been accepted for inclusion in All Theses by an authorized administrator of TigerPrints. For more information, please contact kokeefe@clemson.edu.

AN IN VITRO EVALUATION OF DBM AS
A TISSUE ENGINEERED SCAFFOLD

A Thesis
Presented to
the Graduate School of
Clemson University

In Partial Fulfillment
of the Requirements for the Degree
Master of Science
Bioengineering

by
Stephanie Lorraine Arnold
August 2007

Accepted by:
Karen J.L. Burg, Ph.D., Committee Chair
Ken Webb, Ph.D.
James F. Kellam, M.D.

ABSTRACT

Over 500,000 bone graft procedures are performed each year in the United States. Bone grafting involves a surgical procedure to replace missing bone. Problems can arise with donor and defect sites during and after surgery, sometimes resulting in poor clinical results. The development and optimization of bone graft substitutes via a tissue engineering approach could markedly improve bone graft surgical outcome. Demineralized bone matrix (DBM), a bone graft material, is currently used in a clinical setting but has variable success rates.

The primary objective of the research presented in this thesis was to assess the cellular activity of D1 mouse stromal cells seeded on either partially demineralized bone matrix (PDBM) substrates or completely demineralized bone matrix substrates (CDBM). Before performing a cell-based experiment involving the varying levels of DBM, a study was performed to determine the optimal media conditions for osteoblast formation. Additives β -glycerophosphate and L-ascorbic acid were added to α -MEM media and cultured with D1 cells on DBM to assess the effects of these additives on the rate of cellular differentiation. Significant differences in osteoblast activity were not noted between the two medium conditions.

The final study evaluated cellular activity at four specific time points over a 36 day period after seeding D1 cells on DBM of varying demineralization levels. Based on the assays performed at the four time points, it appears that the D1 cells on the PDBM fragments differentiated toward the osteoblast phenotype and the cellular fragments began to mineralize between 24 and 36 days after initiation of culture, while the cellular

CDBM showed minimal potential for mineralization over the course of the study. Additional studies with more frequent time points are necessary to gain a better understanding of the cellular activity of the D1 cells on the DBM.

DEDICATION

I dedicate this work to my friends and family. The love, support, and encouragement that I received has allowed me to pursue and complete my Master's degree.

ACKNOWLEDGMENTS

I would like to thank my advisor, Dr. Karen J.L. Burg for her guidance, support, and assistance in completing this project. I would also like to thank my committee members, Dr. James Kellam and Dr. Ken Webb for their time, suggestions, and contributions to this work. I would also like to thank the following for their assistance: Dr. Steven Ellis for his help retrieving bone and answering my random questions; Jonathan Campbell and Snowcreek Meat Processing (Seneca, S.C.) for help in retrieving bone samples; Dr. Larry Grimes for his help with statistical analysis; Linda Jenkins for her help with histology; Dr. Chuck Thomas for his assistance with protocols and other questions; LaShan Simpson for her help with atomic absorption spectroscopy and assistance with questions, and finally Dr. Webb for his help with RT-PCR analysis.

I appreciate the support of the Tissue Engineering Laboratory members, especially Cheryl Gomillion, who asked questions, provided me with answers, helped me find answers, and who helped me in numerous ways throughout my research.

This research was supported by the Clemson University Hunter Endowment.

TABLE OF CONTENTS

	Page
TITLE PAGE	i
ABSTRACT	ii
DEDICATION	iv
ACKNOWLEDGMENTS	v
LIST OF TABLES	ix
LIST OF FIGURES	x
AN IN VITRO EVALUATION OF DBM AS A TISSUE ENGINEERED SCAFFOLD	1
LITERATURE REVIEW	1
Introduction	1
Normal Bone Physiology	1
Current Bone Grafts	2
Tissue Engineering	5
Demineralized Bone Matrix	7
Mechanism of Action	11
Limitations of DBM	12
Research Aims	15
MATERIALS AND METHODS	17
Evaluation of Media Cocktails	17
Bone Matrix Preparation	18
Cell Seeding	20
Qualitative Microscopy	23
Cell Viability	23
Histology	24
Real-Time Quantitative Testing	26
Metabolic Activity	26
<i>Lactic Acid and Glucose</i>	26
<i>Alamar Blue</i> [™]	26
Post-Study Quantitative Testing	27
Intracellular Protein	28
Alkaline Phosphatase	29
Extracellular Calcium	31

Table of Contents (Continued)

	Page
Statistical Analysis.....	32
In Vitro Evaluation of DBM	33
Bone Matrix Preparation.....	33
Cell Seeding	35
Qualitative Microscopy.....	38
Cell Viability	38
Histology	38
Real-Time Quantitative Testing	40
Metabolic Activity	40
<i>Lactic Acid and Glucose Levels</i>	40
<i>Alamar Blue</i> [™]	40
Post-Study Quantitative Testing.....	41
Intracellular Protein	41
Alkaline Phosphatase	41
Extracellular Calcium	42
Gene Expression	42
RNA Isolation.....	42
RNA Analysis.....	44
Primer Design	45
Real-Time RT-PCR	48
<i>Amplification Efficiency Determination</i>	50
Statistical Analysis.....	50
RESULTS	51
Evaluation of Media Cocktails.....	51
Bone Matrix Preparation.....	51
Cell Seeding	52
Qualitative Microscopy.....	52
Cell Viability	52
Histology	54
Real-Time Quantitative Testing	58
Metabolic Activity	58
<i>Lactic Acid and Glucose Levels</i>	58
<i>Alamar Blue</i> [™]	60
Post-Study Quantitative Testing.....	61
Intracellular Protein	61
Alkaline Phosphatase	62
Extracellular Calcium	63
In Vitro Evaluation of DBM	65
Bone Matrix Preparation.....	65

Table of Contents (Continued)

	Page
Cell Seeding	66
Qualitative Microscopy.....	66
Cell Viability	66
Histology	69
Real-Time Quantitative Testing	74
Metabolic Activity	74
<i>Lactic Acid and Glucose Levels</i>	74
<i>Alamar Blue</i> [™]	75
Post-Study Quantitative Testing.....	77
Intracellular Protein	77
Alkaline Phosphatase	78
Extracellular Calcium	79
Gene Expression	80
Real-Time RT-PCR	80
DISCUSSION	84
Evaluation of Media Cocktails.....	84
In Vitro evaluation of DBM.....	88
CONCLUSIONS.....	96
RECOMMENDATIONS.....	97
APPENDICES	99
A. H&E Staining Protocol.....	100
B. Von Kossa Staining Protocol for GMA.....	101
C. Primer Design Protocol	102
LITERATURE CITED.....	103

LIST OF TABLES

Table	Page
Table 1 Ethanol dehydration series for histology samples	25
Table 2 IGMA infiltration series for histology samples.....	25
Table 3 BSA dilutants for the standard curve.....	29
Table 4 Dilution scheme for alkaline phosphatase standard curve.....	30
Table 5 Pre-infiltration series.....	39
Table 6 Primers for real-time RT-PCR	47
Table 7 Real-time RT-PCR reaction components.....	49
Table 8 Real-time RT-PCR cyclor conditions	49
Table 9 Bioanalyzer results.....	82
Table 10 Real-time RT-PCR.....	83

LIST OF FIGURES

Figure	Page
Figure 1 An example of tissue engineered bone generation.....	6
Figure 2 Plate and media set-up for the media study	22
Figure 3 Plate set-ups for the level of demineralization study	37
Figure 4 Stereomicroscope images	51
Figure 5 Cell viability.....	53
Figure 6 H&E light micrographs	56
Figure 7 von Kossa light micrographs	57
Figure 8 Cumulative lactic acid production.....	59
Figure 9 Cumulative glucose consumption	60
Figure 10 Metabolic activity via Alamar Blue [™]	61
Figure 11 Intracellular Protein	62
Figure 12 Alkaline phosphatase activity	63
Figure 13 Extracellular calcium.....	64
Figure 14 Stereomicroscope images of bone fragments.....	65
Figure 15 Cell viability.....	68
Figure 16 H&E light micrographs.....	72
Figure 17 Von Kossa light micrographs.....	73
Figure 18 Lactic acid accumulation	74
Figure 19 Cumulative glucose consumption	75
Figure 20 Metabolic activity via Alamar Blue [™]	77
Figure 21 Intracellular protein	78

List of Figures (Continued)

Figure	Page
Figure 22 Alkaline phosphatase activity	79
Figure 23 Extracellular calcium	80

PREFACE

Hundreds of thousands of surgeries are performed each year to treat orthopedic defects in spinal surgeries and in the repair of maxillofacial defects, cranial defects, non-union fractures, tumor removal sites, and in trauma restoration. Autografts are the traditional bone graft but the related surgeries are associated with problems such as donor site morbidity, pain, and infection. As a result, this research is geared toward designing a suitable bone graft substitute that eliminates problems associated with autografts but is as effective as an autograft in inducing bone formation to fill voids in bone tissue.

This thesis provides insight into a tissue engineering approach to developing a novel scaffold for bone grafting. A specific form of allograft is studied during this research - demineralized bone matrix (DBM). Although DBM products are used clinically, variable success rates have been reported. It is believed that some of this variability may stem from inconsistent processing factors of the scaffold. The research presented here focuses on determining a medium cocktail which enhances osteoblast formation and determining the effects of seeding cells on DBM of varying demineralization levels.

To meet the objectives of this research, two primary studies were performed. The first study evaluated the cellular activity of D1 mouse stromal cells seeded on partially DBM scaffolds over a 24 day time period. The activity of cells cultured in two separate medium conditions were compared to each other to determine which allowed the differentiation of the cells towards osteoblasts. The first medium cocktail contained α -MEM with two osteogenic supplements, β -glycerophosphate and L-ascorbic acid. The

second medium contained α -MEM but no osteogenic supplements. Once the most applicable cocktail was discovered in the first study, the cellular activity of D1 cells seeded on partially demineralized and completely demineralized bone scaffolds was observed. The cellular activity of cells was observed over time and histological analyses provided insight into initial mineralization and mineralization that occurred during the course of the study. The work presented represents preliminary research toward the consistent development of demineralized bone matrix as a bone graft substitute for autografts. The results of this research can be used to design and implement future studies.

AN IN VITRO EVALUATION OF DBM AS A TISSUE ENGINEERED SCAFFOLD

LITERATURE REVIEW

Introduction

Approximately 500,000-605,000 bone graft surgeries are performed each year in the United States and approximately 1,000,000 are performed worldwide [1-4]. Bone grafts are used to repair bone defects in orthopedics, dentistry, and neurosurgery. More specifically, bone grafts are used in spinal surgeries and in the repair of maxillofacial defects, cranial defects, non-union fractures, tumor removal sites, and in trauma restoration. In humans, bone is one of the most frequently transplanted tissues [5]. In 2001, the global bone graft market was valued at over one billion dollars and bone graft product sales neared \$15 billion [4].

Normal Bone Physiology

Bone is an important tissue in that it provides protection and structural support to the body. Bone is also involved in the metabolism of minerals and is the primary site for the synthesis of blood cells. Bone maintains its shape and strength via a remodeling process [4]. Normal bone is an organized mineralized structure composed of a matrix and a mineral phase. Amorphous calcium phosphate is the main component of the mineral phase [6] while the matrix portion is composed of type I collagen and osteoid [6]. Osteoid is an organic protein substance, largely composed of type I collagen, that when

deposited is considered to be unmineralized bone matrix [7]. When the osteoid is converted from the organic phase to the inorganic phase, mineralization is thought to occur. Mineralization of bone increases the density but not the volume of the bone [8]. The exact mechanism of mineralization is still unclear.

Bone is modeled during the developmental and growth phases of development. Modeling is achieved by the removal of bone from one site followed by the deposition of new bone at another site while remodeling occurs when mature bone is replaced with new bone. Over a 10 year span, the entire human skeleton is thought to remodel [8]. Osteoclasts and osteoblasts work together as a unit to remodel bone [8]. Bone is removed by osteoclasts via acidification and proteolytic digestion during the process of resorption [8]. Osteoblasts then move into the area where bone was removed and secrete osteoid.

Osteoblasts produce type I collagen as well as many proteins such as osteocalcin, osteonectin, osteopontin, bone sialoprotein, and fibronectin [8]. Osteoblasts regulate calcium and phosphate concentrations so that hydroxyapatite is formed. The process of mineralization of bone is thought to occur once hydroxyapatite is deposited. Osteoblasts also produce large amounts of alkaline phosphatase (ALP), which appears to also play a large role in bone mineralization [8, 9].

Current Bone Grafts

Autologous bone grafts constitute tissue that is removed from the patient and then implanted back into the same patient. Autografts are considered the current gold standard, because the tissue is a perfect match to the patient, there is minimal chance for

an immunogenic reaction [10], and they have the highest success rate of clinically available bone grafts [11]. Autografts contain three essential bone properties that support and induce bone formation: osteoconductivity, osteoinductivity, and osteogenicity [2, 12]. The osteoconductive property of a bone graft refers to the graft's ability to provide structural support and allow the in-growth of blood vessels and bone cells [13]. The ability of a bone graft to induce bone formation via recruitment of precursor osteoblastic cells is termed osteoinduction. When bone grafts are osteoinductive, it is thought that mesenchymal cells are recruited to the scaffold. After reaching the scaffold, the mesenchymal cells have the ability to differentiate into osteoblasts [13]. Osteogenicity is the ability of the bone graft to induce bone formation, due to the presence of precursor stem cells that can differentiate and produce bone directly [14, 15].

Although autologous grafts are the gold standard in bone grafting, there are many drawbacks to this type of graft and affiliated procedure. A limited amount of harvestable bone is available for autograft procedures; the primary donor site is the iliac crest with less frequently tapped donor sites being the distal femur or the proximal tibia [1, 16]. Although the iliac crest is usually a good source of quality cancellous bone, the harvested bone can be difficult to shape since the retrieved bone has variable shape and thickness [2, 17]. Patients who have already had a bone graft surgery may not be good candidates for future autograft procedures. Two surgery sites are required when an autologous bone graft is used, one at the donor site and one at the implantation site. The donor site can be painful, undergo morbidity, as well as become infected, suffer from increased blood loss, have a slow return to normal function [4, 15, 18, 19], and have increased susceptibility to

infection. These disadvantages can lead to higher healthcare costs and longer recovery times for patients [12].

When an alternative to autografts is warranted, allografts can be used instead. Allografts involve the transplantation of tissue from one member of a species to another member of the same species. Currently, cadaver allografts are the most common alternatives used in place of autografts [19]. Unlike the autograft, there is an abundant supply of bone that can be harvested for an allograft procedure [20]. Allografts allow the patient to undergo only one surgery site which can lower the costs involved in the procedure, shorten the hospital stay, and eliminate the problems associated with a second surgical site that evolve from the retrieval of bone for an autograft.

Allografts also have limitations; they are osteoconductive, but not osteoinductive [21, 22]. Allograft bone cannot always initiate osteogenesis; therefore, autograft tissue may be used in conjunction with the allograft tissue [20]. This method re-introduces the problem of a second surgery site that clinicians try to avoid by using allografts instead of autografts. Since the donor bone is explanted from a cadaver, there is a chance of disease transmission from the donor to the patient [19, 23]. Immunological reactions can cause decreased bone formation and can result in immunorejection of the graft [24]. An allograft can also be hard to shape to conform to a bone defect [23]. Each bone graft site is different, therefore it is necessary that a bone graft product be able to readily conform to the damaged area.

Tissue Engineering

Tissue engineering was defined by Langer and Vacanti as an “interdisciplinary field that applies the principles of engineering and life sciences toward the development of biological substitutes that restore, maintain, or improve tissue function or a whole organ” [25]. There are three general strategies for designing tissue engineered devices [25]. The first strategy involves isolating cells from the patient or designing and constructing cell substitutes and then manipulating them to perform a specific function before being placed back into the patient [25]. An advantage to this type of procedure is that surgical procedures are eliminated and that only cells that supply a specific function are replaced. One drawback to cell isolation is immunological rejection and failure of the cells to perform their specific function once placed into a patient [25]. The final two strategies for tissue engineering, as described by Langer (1993), are the utilization of tissue-inducing substances and the placement of cells on or in matrices. Common matrices include natural materials and synthetic polymers. The success of tissue engineering necessitates understanding tissue behaviors such as function and regeneration.

The aim of bone tissue engineering is to design and produce a bone substitute that is comparable or superior to an autograft. As the number of bone graft procedures increase, approximately 7-10% each year since 2001, the bone graft market expands as does the need for alternative products that do not have the drawbacks associated with traditional autografts and allografts [16]. The goal of using bone grafts is to allow a bony defect to be filled with bone similar to that of natural tissue by promoting bone formation.

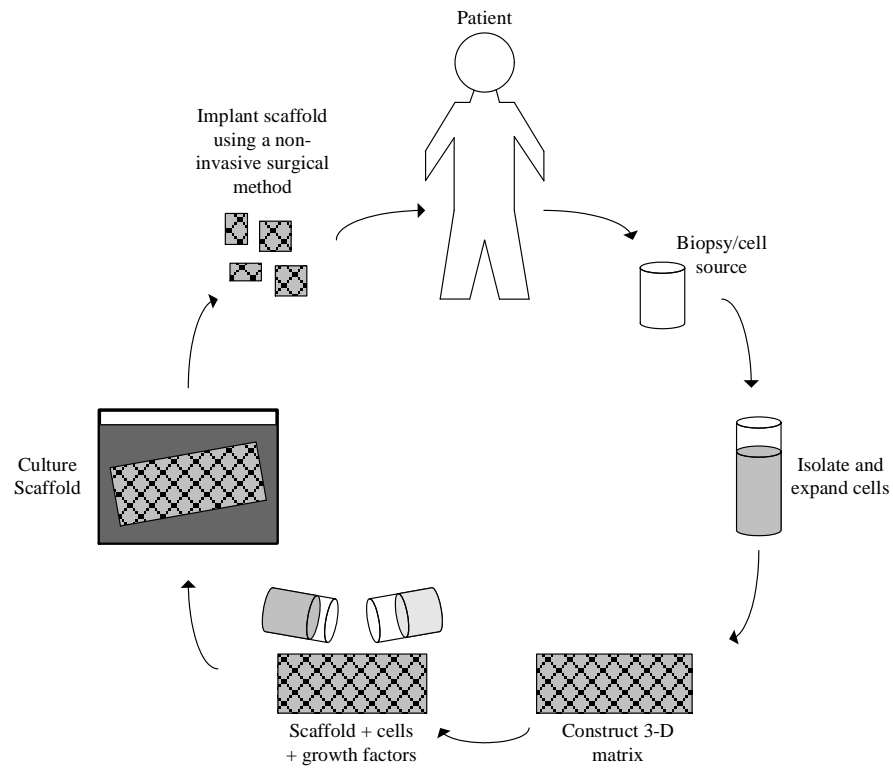


Figure 1 An example of tissue engineered bone generation. A biopsy is removed bone from the patient (or donor in case of an allograft). Cells are isolated from the harvested tissue and constructed into a 3-D matrix. Growth factors and the isolated cells are added to the 3-D matrix and cultured to form a suitable implant. The scaffold is then placed into the patient [13, 26].

Several criteria have been defined by researchers and clinicians as ideal properties of tissue engineered bone grafts. Tissue engineered bone grafts should be free of problems that are associated with autografts and they should shorten recovery times for the patient [16]. Bone grafts should be osteoinductive, osteoconductive, and osteogenic [27]. The scaffold (used interchangeably with matrix in this thesis), should be easily sterilized without the reduction of mechanical or physical characteristics [28]. Ideally, bone graft scaffolds should be biocompatible, absorbable or degradable, highly porous, similar in structure to natural bone, cost-effective, easily manufactured as a commercial product, and easy to handle [2, 16, 28-30]. It is not clear whether or not the scaffold need have mechanical properties similar to natural tissue. Some researchers postulate that this point is not necessary because the primary function of the scaffold is to support bone in-growth, while others believe it is to provide a mechanically stable environment [28].

Demineralized Bone Matrix

Allograft demineralized bone matrix (DBM) may be harvested from a cadaver and, after processing, transplanted into another patient. DBM is prepared by decalcifying bone particles to produce an organic matrix which contains collagen and proteins [15, 19]. The mineral phase is removed by chemicals that chelate or solubilize the mineralized phase [31]. Ethylenediaminetetraacetic acid (EDTA) is an example of a chelating agent that researchers use for demineralization. The drawback to the use of EDTA is that it leaves the matrix devoid of osteoinductive factors [31]. In general, it is

thought that acid solubilization may weaken the overall matrix [31]. HCl, another demineralization agent used by researchers, leaves an osteoinductive matrix [31].

Once implanted into a bony defect in a living body, a successful DBM graft will stimulate bone formation, likely because the organic matrix is preserved during demineralization and the low molecular weight proteins remain in the matrix [19, 32]. These proteins become more accessible as the mineral phase is removed from the bone [2]. Bone morphogenetic proteins (BMPs) and other noncollagenous proteins are believed to recruit and stimulate mesenchymal cell progenitors to differentiate into osteoblasts [32, 33]. It is believed also that DBM contains transforming growth factor-beta, osteogenin, insulin-like growth factor, and fibroblast growth factor; all of which are thought to be involved, either directly or indirectly, in the bone healing cascade [34].

Demineralized bone matrix was reportedly first used in 1889 when Nicholas Senn reconstructed bony defects with decalcified oxen tibia [14, 35]. Following this initial discovery, DBM did not gain the interest of many researchers and clinicians [14, 19, 35] until Urist implanted acid demineralized bone into extraskeletal sites, resulting in the development of bone ossicles (1965). Two years later, Dubuc and Urist showed that even when bone fragments are surface decalcified, bone induction occurs [36]. The bone induction principle is the manner by which new bone is formed by the attraction of mesenchymal stem cells (MSCs) but not by recalcification of the implanted bone graft. In the same *in vivo* study, it was demonstrated that prolonged exposure of bone fragments to HCl, saline and 70% ethanol causes the bone induction principle to be void. It was also seen that the surfaced demineralized bone fragments, which were demineralized in

0.5 N HCl for 1-2 hours, had a larger amount of new bone formation than the completely demineralized bone fragments which were in 0.5 N HCl for 1 week [37]. It has been suggested that this outcome might be caused by a high number of macrophages and giant cells destroying the completely demineralized bone graft. Duboc and Urist also suggest that completely demineralized bone fragments might allow bone formation via the bone induction principle more rapidly than what is desired [37]. The theory proposed by Duboc and Urist about completely demineralized bone fragments was later corroborated by Shih in 2005 when he suggested that the mineral in partially demineralized bone may dissolve slowly, allowing a slow and steady release of BMP's, while CDBM released the BMPs at a faster rate [38]. It was noted in the 1960's that when demineralization factors such as the exposure time, the ambient temperature, and the concentration of HCl were controlled there was consistent osteoinduction by the decalcified bone [39]. In 1970, Urist and Strates reported, in a study involving implantation of DBM in rabbits, that the amount of demineralization was directly proportional to the amount of bone formation. In separate studies in the 1960's and 1970's, it was demonstrated that diaphyseal bone from the humerus, femur, tibia, and the fibula showed high levels of osteoinduction while other soft tissues such as the pelvis, scapula, and all cartilage (except costal rabbit cartilage) showed little to no osteoinductive properties [39]. In 1979, Urist discovered BMPs, which are considered the DBM's main bone induction agent [39]. Zhang reported in 1997 that bone decalcified to a 2% residual calcium level had a higher amount of osteoinductivity than fragments with either higher or lower amounts of residual calcium. Bone fragments were demineralized in 0.5 N HCl for 180 minutes to reach this level (2%)

of residual calcium. It was also noted that as the residual calcium level decreased from 32.7% to 2%, the osteoinductivity increased in the *in vivo* model studied. As the residual calcium level decreased below 2%, the level of osteoinductivity was lower than that observed of the DBM fragments with 2% residual calcium. DBM has also shown promising results clinically. In 1999, Russell and Block evaluated results from 21 clinical cases in which DBM was used as a bone graft and reported that 80% of these cases had successful outcomes [21].

DBM can be loaded with other products in order to maximize bone formation. In 2001, Gitelis and coworkers showed that 42 out of 44 bone repair patients had greater than 80% bone repair when a graft composed of DBM and calcium sulfate was used [14]. Four years later, Mauney seeded bone marrow stromal cells (BMCs) on DBM of various demineralization levels. The results showed that fragments with partially demineralized bone (PDBM) had the highest frequency of bone formation when implanted into athymic female mice, while fully demineralized and fully mineralized bone fragments showed the same frequency of bone formation, but lower than that of the PDBM [33]. Mauney also suggested that when bone is over demineralized the osteogenic factors are removed and the hydroxyapatite nucleation sites, which are essential for new bone formation, may be depleted [33]. In 2005, Thomas reported that while using an *in vitro* model comparing surface demineralized, partially demineralized, and completely demineralized bone fragments, no difference in the cellular activity between the fragment types was observed, although osteoblast formation was noted on all substrates [13]. This observation may be

attributed to the procedures that were followed or because the *in vitro* study that was used was not accurate enough to obtain results similar to those received in *in vivo* studies.

DBM is successful because it contains osteoinductive and osteoconductive properties. DBM is biocompatible, biodegradable, cost effective, and readily available [18, 40, 41]. DBM stimulates revascularization quickly, allowing bone formation in a timely manner [42]. Urist reported that when bone fragments were decalcified in 0.5 N HCl and implanted into an extraskeletal site, bone formation consistently occurred 25 days after the operation [43]. The demineralization process destroys antigenic substances that are present in the bone [40, 41]. Pathogens are likely also destroyed during the processing of the DBM [24]; one manufacturer reported that in 1.5 million procedures involving one type of DBM, there were not any reported cases of infectious diseases transmission [42]. A large tissue bank with over 20,000 donors also reported no disease transmission [42]. These statistics suggest that DBM may provide a superior bone graft substitute as compared with traditional allografts because DBM is less likely to invoke an immune response.

Mechanism of Action

It is believed that DBM does not recalcify when implanted into muscle; rather, the DBM produces new bone via induction [36, 44]. Bone induction leads to the development of lamellar bone as well as the recruitment of new marrow cells [36]. The bone induction process that occurs in response to implantation of DBM can be broken down into four events [39]. Although the exact timing of these events varies between

studies, the general timing and order of the mechanism is similar. After the inflammatory phase is initiated on Day 1 following implantation of DBM, MSCs migrate into the matrix within 2 days of implantation during this initial event. Event 2 occurs between the 2nd and 18th days, when the MSCs differentiate into giant cells and chondrocytes [39, 45]. The third event involves the development of cartilage in poorly vascularized areas between Days 8 and 20 and the formation of woven bone in vascularized areas of the matrix between the tenth and twentieth days [39]. Calcification of the cartilage matrix begins by Day 11 or 12 and is subsequently followed by chondrolysis (dissolution of cartilage) [45]. The cartilage tissue is eventually replaced by osseous tissue [45]. The final event includes the production of bone marrow between Days 20 and 30 [39, 46].

Limitations of DBM

It has been reported that clinical results describing DBM application have been highly variable. One possible reason for failure is that the graft material causes an inflammatory response which accelerates graft degradation and subsequently leads to premature degradation and failure of the graft [47]. It is also believed that the non-uniformity in the processing of the DBM by bone banks and commercial suppliers leads to variable clinical results [2, 12, 46, 48]. DBM is denatured at temperatures above 45°C so any processing technique which causes an increase in temperature above 45°C can have detrimental impacts on the overall ability of DBM to induce bone formation [41]. The osteoinductive and osteogenic levels of DBM may be affected by the donor gender, donor age, medical status of the donor at death, length of time before the bone is

harvested from the donor, implantation site, size of the bone fragments, geometry of the bone fragments, amount of demineralization, and the storage conditions [42, 48-51]. It is also possible that the osteoinductivity levels of DBM vary between species which would explain why the success levels in humans and animals differ [50].

Sterilization procedures can also affect the osteoinductive properties of DBM. The most common methods researched include ethylene oxide (EtO), autoclave, and gamma radiation. EtO can react with water and chloride ions to form a toxic compound, ethylene chlorohydrin (ECH) [47]. This reaction can occur if the graft material still contains residual ethylene oxide components after sterilization; however, exposure to vacuum minimizes this risk [24]. DBM should not be autoclaved before implantation because the osteoinductive potential will be destroyed [39]. Gamma radiation has shown that even when it is used to sterilize DBM, the DBM is still viable although some believe that new bone formation is dependant on the dose of gamma radiation [24, 39]. Ethanol is a disinfectant, not a sterilant, because it does not kill spores and certain viruses [39]. Therefore, EtO and gamma radiation are considered to be the most effective DBM sterilants.

The non-uniformity of processing bone grafts, the donor status at the time of harvest, the size and shape of the bone graft, the amount of demineralization and the sterilization procedures all have the ability of affecting the clinical outcomes of the bone graft [22]. Schwartz studied demineralized freeze-dried bone allografts (DFDBA), with fragment sizes of 200-500 microns, from six bone banks to determine their ability to induce bone formation [50]. Fragments from select bone banks demonstrated

osteoinductive properties while DBM from other bone banks did not. Testing of two different batches from the same bone bank showed high variability, where one set of DBM showed osteoinductive tendencies while the other did not [50]. This study showed that the different processing procedures employed by bone banks affects the osteoinductive properties of DBM, and that DBM from the same bone bank also differs in its ability to induce bone formation [50]. It has also been suggested that the bone fragment processing variables produce far greater widespread distribution in the clinical outcomes of DBM than can be attributed to the bone source [22].

As bone particles undergo demineralization, they lose some of their structural strength as the mineral phase of the bone is removed [2]. Depending on the form of DBM used, the DBM can be hard to handle and place into a bone defect site [19]. When used as a powder, DBM has a tendency to migrate from the graft site due to bleeding [19]. To minimize these problems, DBM is often supplied as a gel, a putty, flexible strips, a moldable paste with bone chips, or an injectable bone paste [2]. The osteoinductive properties of DBM is enhanced in clinical and research settings by creating a gel from bone chips with the addition of either glycerol, hyaluronic acid, or poloxamer 407 [19]. Bone marrow cells seeded on DBM appear to accelerate bone healing in rats.

Current research methods are expensive and use many *in vivo* studies. Until recent years, bone tissue engineering has focused on *in vivo* models and, to a lesser extent, *in vitro* models [52]. *In vitro* models can be used to screen implants before insertion into an animal and to optimize conditions for bone tissue engineering

applications [52]. *In vitro* models are also used to evaluate the effects of various implant properties, such as scaffold composition and architecture, cell-seeding density, and length of culture on cell growth and development [52]. *In vivo* testing explores the overall biocompatibility of the implant material. There is a need to design and implement *in vitro* models for bone tissue engineered implants that accurately resemble the *in vivo* environment. Such models would help optimize constructs before testing in animals, which would reduce the cost and number of animals needed for *in vivo* studies. Currently, there is not an accurate *in vitro* model that can be used in studies involving DBM to predict *in vivo* behavior.

Research Aims

Currently, DBM is a solution to problems associated with autografts and allografts in a clinical setting [24]. DBM has been used successfully in clinical surgeries such as revision arthroplasty, spinal fusion, non-union fractures, dental augmentation, craniofacial defects, joint surgery, and as a graft substitute [19, 22]. Although DBM is used increasingly each year, it is not an optimal autograft bone substitute due to variability in the clinical success rate of the DBM related procedures.

As the need for alternatives to autografts and allografts continue to increase, the need to optimize tissue engineered grafts also continues to increase. Since processing factors contribute highly to the variability in the success rate of demineralized bone matrix products, it is vital that research is completed to determine the effects these factors have on the ability of DBM to stimulate bone formation.

The goal of this research was to perform an *in vitro* analysis to determine the effects of cellular activity when cells are seeded on demineralized bone matrices of varying mineralization levels. A protocol previously used by Thomas [13] was employed to defat bone fragments in a mixture of chloroform and methanol, demineralize the fragments in 0.5 N HCl, lyophilize the fragments, and sterilize them in ethylene oxide. The bone was seeded with cells and the cellular activity was observed. A preliminary study was completed to determine if additives that were added to the media for *in vitro* studies involving DBM, specifically L-ascorbic acid and β -glycerophosphate, improve the ability of the cells to differentiate towards osteoblasts. This study was completed by comparing partially demineralized bone seeded with cells with two types of media: media containing the differentiation additives and media without these additives. The overall objective of the research was thus to determine the effects of a specific processing factor, the level of demineralization of the bone fragments. The cellular activity of cells seeded on partially demineralized bone fragments were compared to the cellular activity of bone fragments that were completely demineralized. All other processing factors remained the same during this study.

MATERIALS AND METHODS

Two studies were performed in order to meet the specified objectives of this research. The first study entailed seeding cells onto partially demineralized bone fragments and studying two medium conditions. A second study was performed to evaluate the effects of the demineralization level on cellular activity over time, after development and optimization of the methods for demineralization of the bone fragments and analysis of the cell culture between the two medium conditions,. In both studies, microscopic images were captured to assess cellular attachment, real-time quantitative testing was carried out to gain an overall understanding of the metabolic activity of the cells in culture, and post-study testing was conducted to monitor differentiation of the cells and the mineralization of the bone. The expression of osteoblastic genes in the cell culture was monitored in the final study.

Evaluation of Media Cocktails

The purpose of the first phase of this research was to examine the effects of osteogenic supplements added to medium to culture cells seeded on DBM. DBM is synonymous with scaffold for the rest of this publication. Substrate preparation was modified from a previous protocol [13]. The cell culture was evaluated to determine if osteogenic supplements affect the activities of cells seeded on DBM.

Bone Matrix Preparation

A modified version of Urist's protocol [13] was used to defat and demineralize bovine bone. Diaphyseal cortical sections of bovine femurs were obtained from two freshly slaughtered cows from the Clemson University Meat Lab (Clemson, SC). Cow carcasses were stored at approximately 2.2°C for 14-21 days before the femurs were removed. Once the femurs were obtained, tissue was removed from the diaphyseal section and then frozen at -80°C. A total of two femurs were obtained from two cows on separate processing dates. The bone was sectioned with a band saw and cut into pieces approximately 1 cm x 1 cm x 2 cm (Delta Machinery, Jackson, TN) and then frozen at -80°C. Sectioned bone from two cows was added to an A 11 basic Analytical mill (IKA[®] Works, Wilmington, NC) to grind the bone. Fragments in the range of 0.86 - 1.91 mm were collected using a Collector[®] Tissue Sieve System (PGD Scientifics, Frederick, MD) with mesh screens of size 20 and 10, respectfully. A total of 26 mL of ground cortical bone was collected.

Bone fragments were added to a glass bottle containing a defatting solution which consisted of a 3:1 volume of a chloroform/methanol solution (58.5 mL of chloroform (Acros, NJ) and 19.5 mL of methanol (Fisher Scientific, Fairlawn, NJ)). The glass bottle was sealed with a top and the contents were stirred at 4°C for two hours. The spent liquid was removed and 58.5 mL fresh defatting solution was added to the glass bottle and the process was performed a second time. After the second removal of the defatting solution, the bone fragments were washed in one volume (26 mL) of 100% ethanol for 30 minutes

at 4°C; the ethanol was then removed and the fragments were placed in a clean glass bottle and stored at 4°C for approximately 11 hours.

The bone fragments were demineralized in ten volumes of 0.5 *N* HCl (260 mL) (Fisher Scientific) at room temperature. The solution was stirred continuously at 40 minute intervals. Stereomicroscopy was performed to determine the level of demineralization after each 40 minute cycle using an EMZ stereomicroscope (Meiji Techno, San Jose, California). Digital images of bone fragments were captured using a SPOT INSIGHT digital color camera and software (Diagnostic Instruments, Sterling Heights, MI) and analyzed with Image-Pro Plus 4.5 Software (Media Cybernetics, Bethesda, MD). The remaining fragments were washed with large volumes of distilled water to neutralize the remaining acid and to remove any mineral residue. Partially demineralized bone fragments (PDBM) were obtained following two 40 minute acid cycles.

A negative control (NDBM) was prepared by adding approximately 5.5 mL of PDBM to 40 mL of guanidine hydrochloride (GnHCl) in 50 mM Tris buffer (pH 7.4) (both from Sigma, St. Louis, MO) to inactivate the osteoinductive proteins. The solution was stirred at 4°C for 16.5 hours and then rinsed in distilled water at room temperature.

The activity of the osteoinductive proteins in the bone fragments was preserved by lyophilizing the fragments [36, 53] with a BenchTop “K” Series freeze dryer (VirTis, Cardiner, NY). The bone fragments were sterilized at room temperature in a 12-hour ethylene oxide (EtO) infiltration cycle in an AN74i sterilization chamber (Andersen Products, Haw River, NC) followed by two hours of degassing in the same chamber. The

samples were placed in a dessicator for 57 hours under vacuum (500 mm Hg) until conditioning.

Cell Seeding

One day prior to cell seeding, the sterilized bone fragments were conditioned in sterile 50 mL centrifuge tubes to ensure all residual HCl was removed. The fragments were washed twice in 10 minute intervals in sterile phosphate buffered saline (PBS) (Sigma). The wash was immediately followed by five 30-minutes rinses and one 12-hour rinse in Minimum Essential Medium (α -MEM) (Invitrogen, Carlsbad, CA) supplemented with 10% fetal bovine serum (FBS) (Mediatech, Herdon, VA) and 1.0% Antibiotic-Antimycotic (Invitrogen). This supplemented medium will be denoted as α -MEM-C. The medium contains phenol red which changes color with change in local acidity. The medium will appear orange to yellow as the pH decreases

While the conditioning process was conducted, twelve tissue culture grade 24-well plates (Costar, Corning, NY) were coated with Sigmacote[®] (Sigma) to form a hydrophobic surface on the bottom of each well. The plates were left to dry in a sterile hood for two hours. Days 4, 13, and 24 were selected as time points at which to monitor changes in cell differentiation. Four 24-well plates were set up per time point; therefore, a total of 12 plates were used for the media study.

After the conditioning cycle was completed, fresh medium was added to each set of bone fragments. The tips of glass pipets were modified with a band saw to allow a wider tip for bone fragment transfer. The modified EtO sterilized pipets were used to

transfer 0.1 mL aliquots of bone fragments to corresponding wells, as portrayed in Figure 2. One mL of fresh α -MEM-C was then added to each well. The well plates were placed in a sterile hood overnight.

Osteogenic supplements consisting of 10 mM β -glycerophosphate and 50 μ g/mL ascorbic acid (both from Sigma) were added to α -MEM-C to form α -MEM-M. The spent media was aspirated from the well plates on the day of cell seeding, and replaced with 1 mL of either α -MEM-C or α -MEM-M, as displayed in Figure 2. Multipotent mouse marrow stromal cells (D1's) (#CRL-12424, ATCC, Manassas, VA) were seeded into each well at a density of 3×10^5 cells/well at passage 33. The negative control group received bone fragments and medium, but no cells. All well plates were placed in an incubator under standard conditions of 37°C and 5% CO₂ on an orbital plate (IKA[®] Works), shaking at a speed of approximately 50 rpm. The day of cell seeding was denoted as Day 0 of the study. The media was changed on Days 2, 4, 6, 8, 10, 12, 13, 15, 17, 19, 21, and 23 during the 24-day study.

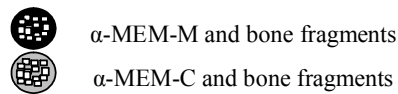
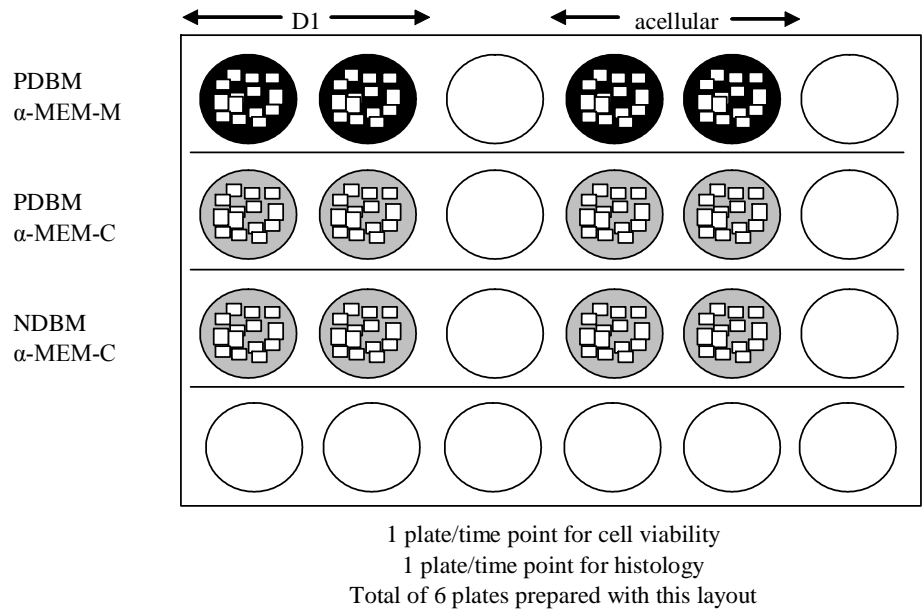
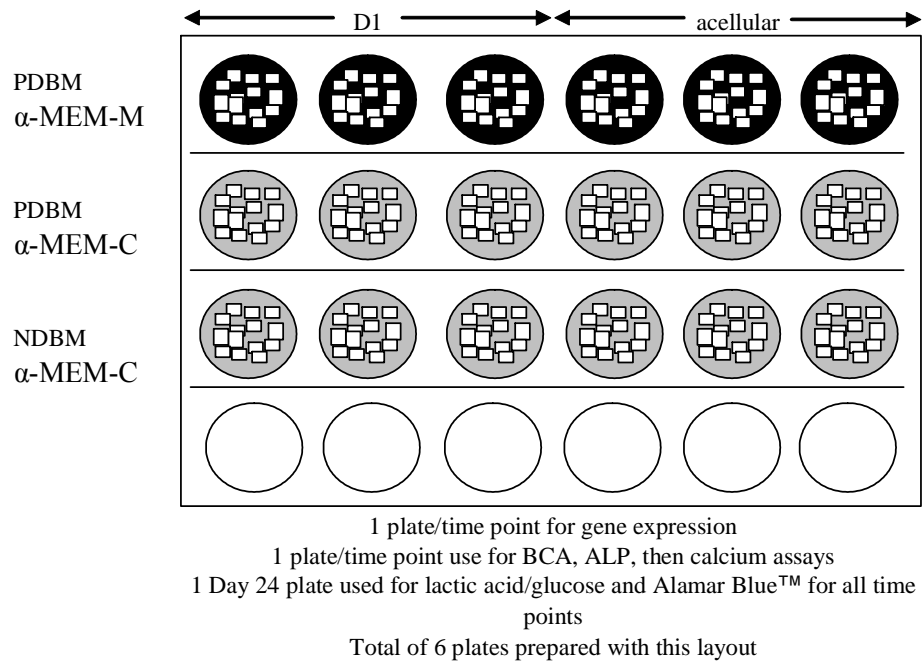


Figure 2 Plate and media set-up for the media study

Qualitative Microscopy

Cell Viability

A LIVE/DEAD[®] Viability/Cytotoxicity kit (Molecular Probes, Eugene, OR) was employed according to the manufacturer's protocol to analyze the cells on the bone fragments and to determine if the media conditions affected the viability of the cells on Days 4, 13, and 24. Working solutions were formed by adding 20 μ L 2 mM Ethidium-homodimer-1 (EthD-1) and 5 μ L of 4mM calcein AM to 10 mL of sterile PBS in a sterile 15 mL centrifuge tube. All bone fragments specified for this assay were moved to fresh sterile 24-well plates and then rinsed in sterile PBS to remove any residual medium. The PBS was aspirated and one mL of the working solution was added to each well. The plates were incubated for 45 minutes at room temperature in a place void of light. Images were captured using an Axiovert 135 microscope (Zeiss, Thornwood, NY), a ProgRes[™] C10^{Plus} digital color camera and ProgRes Capture Basic 1.2 software (both from Jenoptik, Jena, Germany). The images were analyzed with Image-Pro Plus 5.1 Software (Media Cybernetics). The cells were fluorescently labeled using the calcein AM and ethidium homodimer dyes in the kit and following the manufacturer's protocol. Live cells retain a dye that produces bright green fluorescence (excitation and emission of 495 nm and 515 nm, respectively), while dead cells fluoresce a bright red (excitation of 495 nm and emission of 635 nm).

Histology

Samples from Days 4, 13, and 24 were analyzed using histological techniques. At each specified time point, the fragments were rinsed twice in sterile PBS (Sigma) and then fixed overnight in 10% neutral buffered formalin at 4°C. Samples were placed in a Tissue Tek™ VIP automatic tissue processor (Miles Scientific, Mishawaka, IN) and processed with a 24-hour dehydration cycle in ethanol, as shown in Table 1. Samples were infiltrated under vacuum (500 mm Hg) in ascending concentrations of Immuno-Bed modified glycol methacrylate (I-GMA) (Polysciences, Warrington, PA) as detailed in Table 2. After two cycles in 100% IGMA, the samples were blotted dry and transferred to embedding trays. The samples were embedded with fresh IGMA according to the manufacturer's protocol and then stored in a dessicator under vacuum (500 mm HG) at 4°C. Samples were placed in a 35°C oven to complete the hardening process and stored in a dessicator at room temperature until sectioning. Eight micrometer sections were obtained using a RM2155 rotary microtome (Leica, Bannockburn, IL). Sections were stained with hemotoxylin and eosin (H&E) and von Kossa to study the cellular attachment on the bone fragments as well as the mineralization of the bone, respectively. Protocols can be found in Appendices A and B. Images were captured using an Axiovert 135 microscope (Zeiss), a ProgRes™ C10^{Plus} digital color camera and ProgRes Capture Basic 1.2 software (both from Jenoptik). The images were analyzed with Image-Pro Plus 5.1 Software (Media Cybernetics).

Table 1 Ethanol dehydration series for histology samples

Percent EtOH	Time (hours)
70	2
80	2
95	3
95	5
100	5
100	7

Table 2 IGMA infiltration series for histology samples

Percent I-GMA	Time (hours)
10	≥ 24
20	≥ 24
30	≥ 24
40	≥ 24
50	≥ 24
60	≥ 24
70	≥ 24
80	≥ 24
90	≥ 24
100	≥ 24
100	≥ 24

Real-Time Quantitative Testing

Metabolic Activity

Lactic Acid and Glucose

The lactic acid and glucose levels were analyzed before every medium change and on the last day of the study, which occurred on Days 2, 4, 6, 8, 10, 12, 13, 15, 17, 19, 21, 23, and 24. Before the medium was aspirated, 200 μL of spent media was removed from each well and analyzed using a YSI 2700 SELECT™ biochemistry analyzer (YSI, Yellow Springs, OH). The analyzer determines the glucose and lactic acid concentrations simultaneously via an immobilized enzyme membrane technology. Specifically, a sipper withdraws 25 μL of each medium aliquot and deposits it in a chamber where it is stirred and diluted with buffer. The buffer/aliquot mixture diffuses through a polycarbonate membrane and contacts a thin layer of an oxidase enzyme (L-lactate oxidase for lactic acid and glucose oxidase for glucose). Upon contact, a hydrogen peroxide (H_2O_2) product is formed. H_2O_2 then diffuses toward a platinum anode which causes a current to be produced at an electrochemical probe. The current value is compared to calibration values and the concentration of both substrates is given.

Alamar Blue™

The metabolic activity of the cells seeded on the demineralized bone fragments was assessed on Days 4, 13, and 24 using an Alamar Blue™ dye (BioSource International, Carmarillo, CA). The spent media was aspirated at these time points, and replaced with

either fresh α -MEM-C or α -MEM-M after aliquots were removed for lactic acid and glucose level determination. The well-plates were placed in an incubator at 37°C and 5% CO₂ for four hours. Alamar Blue™ dye was added in 100 μ L quantities to each well before the particular well plate was placed back in the incubator for an additional three hours to allow uptake of the dye into the metabolically active cells. Medium aliquots were transferred in triplicate to a black 96-well plate (Corning). The fluorescence values were read on a SpectraMax® Gemini EM Dual scanning spectrofluorometer (Molecular Devices, Sunnyvale, CA). The excitation and emission filters were 544 nm and 590 nm, respectively. As the nonfluorescent blue dye undergoes reduction in metabolically active cultures, the dye become pink and fluorescent which allows visual observation of change in the level of metabolic activity of the cells. This assay is not endpoint assay, therefore the remaining medium in the 24-well plates was aspirated and replaced with 1 mL of fresh medium. Results from this assay and the lactic acid and glucose assays were used to assess cellular metabolic activity.

Post-Study Quantitative Testing

The 24-well plate specified for post-study quantitative testing at each time point was rinsed twice in sterile PBS (Sigma). Following the rinse, 1 mL of 0.5% Triton-X (Fisher Scientific) in PBS (Sigma) was immediately dispensed in the plates. The plates were frozen at -80°C until the plates for all time points were collected. The plates underwent three freeze/thaw cycles to lyse and release the proteins from the scaffolds in

preparation for alkaline phosphatase and intracellular protein assays. The remaining cell lysate and bone fragments were reserved for the extracellular calcium assay.

Intracellular Protein

The intracellular protein content was determined using a BCA Protein Assay Reagent Kit (Pierce Biotechnology, Rockford, IL) and following the manufacturer's protocol. BSA standards were prepared in a 24-well plate using deionized water as a dilutant as shown in Table 3. A working reagent (WR) was prepared by mixing Reagent A with Reagent B (50A:1B) to form a clear-green WR solution. A 96-well plate (Corning) was prepared for sample analysis by transferring 25 μ L of each standard and sample into separate wells in triplicate before adding 200 μ L of the working reagent to each well. The plate was gently shaken on a shaker plate (IKA[®] Works) for 30 seconds before being placed in an incubator at 37°C for 30 minutes. At the end of incubation, the plate was cooled for 10 minutes at room temperature. The absorbance values were measured at a wavelength of 562 nm on an MRX[®] Revelation absorbance microplate reader (DYNEX Technologies, Chantilly, VA). A standard curve was constructed by plotting the average blank readings for each BSA standard against its concentration in μ g/mL. Linear regression was performed on the standard curve and was used to determine the protein concentration for each sample. This data was used to normalize results from the alkaline phosphatase and extracellular calcium assays.

Table 3 BSA dilutants for the standard curve

Plate Well	Diluent Volume	BSA volume & source	Final conc.
A	0	300 μ L stock	2000 μ g/mL
B	125	375 μ L stock	1500 μ g/mL
C	325	325 μ L stock	1000 μ g/mL
D	175	175 μ L from B	750 μ g/mL
E	325	325 μ L from C	500 μ g/mL
F	325	325 μ L from E	250 μ g/mL
G	325	325 μ L from F	125 μ g/mL
H	400	100 μ L from G	25 μ g/mL
I	400	0	0 (Blank)

Alkaline Phosphatase

The alkaline phosphatase content of each sample was determined according to manufacturer protocol from Kit #104 (Sigma). A diluted p-nitrophenol (Sigma) standard solution was formed by diluting p-nitrophenol in 0.02 *N* NaOH (Fisher Scientific). A standard curve was generated using the dilution scheme displayed in Table 4. The diluted p-nitrophenol samples were pipetted in triplicate in 200 μ L quantities into a 96-well plate (Corning) in order to generate a standard curve. The absorbance was read at 410 nm and the standard curve was determined by plotting absorbance versus ALP activity. Linear regression was performed and the equation used to determine the ALP activity in the samples. A working reagent was prepared by adding phosphatase substrate solution and alkaline buffer solution 1:1 (both from Sigma). The working reagent was added to 18 wells in a 24-well plate (Corning) in 500 μ L quantities and allowed to incubate at 37°C for 15 minutes. Cell lysates from the post-study testing plates were

added in 100 μL quantities to separate wells containing the working reagent. A volume in the amount of 100 μL of deionized water was added to the control well. The plates were mixed on an orbital IKA[®] shaker (IKA[®] Works) for 30 seconds before being placed in an incubator for 30 minutes at 37°C. The reaction was stopped by adding 1.5 mL of 0.25 N NaOH (Fisher Scientific) and mixing for 30 seconds on an orbital IKA[®] shaker. The contents were transferred in triplicate in 200 μL quantities to a 96-well plate (Corning). The absorbance was measured at 410 nm using a MRX[®] Revelation absorbance microplate reader. The concentration of each sample was determined by using the quadratic equation from the standard curve. The ALP activity was normalized with the total intracellular protein content. The basis of this assay is that a yellow colored *p*-nitrophenol product is generated as ALP hydrolyzes the *p*-nitrophenol phosphate in an alkaline cell lysate.

Table 4 Dilution scheme for alkaline phosphatase standard curve

Tube #	Diluted <i>p</i> -nitrophenol solution (mL)	0.02N NaOH (mL)
1	1	10
2	2	9
3	4	7
4	6	5
5	8	3
6	10	1

Extracellular Calcium

The remaining bone fragments and cell lysates were reserved to determine the extracellular calcium content. A 6 *N* HCl sample solution was composed by transferring the remaining contents of each sample well to individual glass test tubes (VWR International, West Chester, PA) and adding 1 mL of ULTREX[®] II Ultrapure 12 *N* HCl (J.T. Baker, Phillipsburg, NJ). The tubes were placed in I-CHEM[™] glass bottles (Chase Scientific Glass, Rockwood, TN) that contained 20 mL of 6 *N* HCl. The glass bottles were sealed with Teflon[®]-lined lids and placed in a water bath. After bringing the water to a boil, samples were heated for an additional 6 hours in order to dissolve the bone fragments. After all the samples were dissolved, each test tube was placed under nitrogen gas flow in order to evaporate the supernatant. A precipitate remained in the bottom of each test tube. One mL of Ultrapure 0.01 *N* HCl was added to each test tube to bring the dried precipitate into solution. Each sample was vortexed and transferred to 1.5 microcentrifuge tubes (VWR International, West Chester, PA) and frozen at -20°C. After thawing the samples, 1.98 mL of an atomic absorption matrix solution was added to 0.02 mL of sample to eliminate chemical interference from phosphorus. The matrix solution consisted of 0.3 *N* Ultrapure HCl and 0.5% (w/v) lanthanum oxide (Alfa Aesar, Ward Hill, MA). Standards of 5, 15, and 30 µg/mL of Ca²⁺ were prepared from a calcium reference solution (Fisher Scientific) and used to calibrate the Perkin Elmer 3030 atomic absorption flame spectrophotometer (Perkin Elmer Instruments, Wellesley, MA). The samples were run in triplicate on the same piece of equipment. The total extracellular calcium was normalized with the intracellular protein content. The basis of this assay is

that the calcium ions are atomized when heated by a flame. The ions are reduced to unexcited, ground state atoms which absorb light at a wavelength of 422.7 nm (specific for calcium).

Statistical Analysis

All quantitative assays were executed in triplicate. Statistical analysis was performed using SAS[®] System 9.1 statistical software (SAS Institute Inc., Cary, NC, USA). The Least Squares Mean (LSMEANS) method was used for all quantitative assays to determine the effects of the medium on the cellular activity of D1 cells seeded on DBM. Values are represented by a standard error of mean (SEM) of $n = 3$. A significance level of $p = 0.05$ was employed for all comparisons.

In Vitro Evaluation of DBM

The final phase of this research was to examine the effects of partially demineralized bone fragments and completely demineralized fragments on cellular activity over 36 days. An evaluation of the cellular bone fragments was conducted to determine the differences of cellular activity over time for each type of bone fragment.

Bone Matrix Preparation

A modified version of Urist's protocol [13] was used to defat and demineralize bovine bone. Diaphyseal cortical sections of bovine femurs were obtained from freshly slaughtered cows from the Snow Creek Meat Processing Facility (Seneca, SC) for the final study. The cow carcasses were stored at approximately 2.2°C for 21-28 days before the femurs were removed. Three femurs were obtained from Snow Creek to ensure that bone was obtained from at least two cows. The bone was transferred on ice and immediately placed in a -80°C freezer. After freezing, tissue was removed from the diaphyseal section of the femurs and then frozen at -80°C. The bone was sectioned with a band saw (Delta) and cut into pieces approximately 2 cm x 2 cm x 2 cm and then refrozen at -80°C. The bone was sectioned into pieces 1 x 1 x 1 cm with a dremel (Dremel, Racine, WI). The bone was then placed in a rotor-speed mill (Fritsch, Idar-Oberstein, Germany) with a sieve insert of 2 mm. Approximately 35 mL of ground cortical bone was collected from the three femurs for defatting and demineralization.

Bone fragments were placed in a glass bottle along with a defatting solution which consisted of a 3:1 volume of chloroform/methanol solution (90 mL of chloroform (Acros, NJ) and 30 mL of methanol (Fisher Scientific)). The glass bottle was sealed with a top and the contents were stirred at 4°C for two hours. The spent liquid was removed and an additional 120 mL of fresh defatting solution was added to the glass bottle and the process was performed a second time. After the second removal of the defatting solution, the bone fragments were washed in one volume (40 mL) of 100% ethanol for 30 minutes at 4°C, the ethanol was removed, and the fragments were placed in a clean glass bottle and stored at 4°C for approximately 9 hours.

The bone fragments were demineralized in ten volumes of 0.5 *N* HCl (350 mL for 80 minutes and 250 mL for the remaining 120 minutes) (Fisher Scientific) at room temperature. The solution was stirred continuously in 40 minute intervals. Following each 40 minute time period, a calcium oxalate test was performed and a visual analysis by stereomicroscopy was conducted to determine the end point of demineralization. After each acid cycle, 5 mL of spent HCl was combined with 5 mL of 5% (v/v) ammonium hydroxide and 5 mL of 5% (v/v) ammonium oxalate (both from Fisher Scientific) to chemically determine when bone fragments were completely demineralized. Stereomicroscopy of the samples was performed at the end of each acid cycle as described previously. Partially demineralized bone fragments were obtained following two 40 minute cycles, and completely demineralized bone fragments were obtained after 200 minutes in the demineralization solution.

A negative control (NDBM) was prepared by adding approximately 6 mL of CDBM to 40 mL of guanidine hydrochloride (GnHCl) in 50 mM Tris buffer (pH 7.4) (both from Sigma) to inactivate the osteoinductive proteins. The solution was stirred at 4°C for 16 hours followed by two rinses in distilled water at room temperature.

The activity of the osteoinductive proteins in the PDBM and CDBM fragments was preserved by lyophilizing the fragments in a Labanco Lyph-Lock 6 freeze dryer (Labanco Corporation, Kansas City, Missouri). Before lyophilization, fragments were stored at -20°C for 30 minutes. The bone fragments were then sterilized at room temperature during a 12-hour ethylene oxide (EtO) infiltration cycle in an AN74i sterilization chamber (Andersen Products), and degassed for two hours in the same chamber. The samples were placed in a dessicator for 152 hours under vacuum (500 mm Hg).

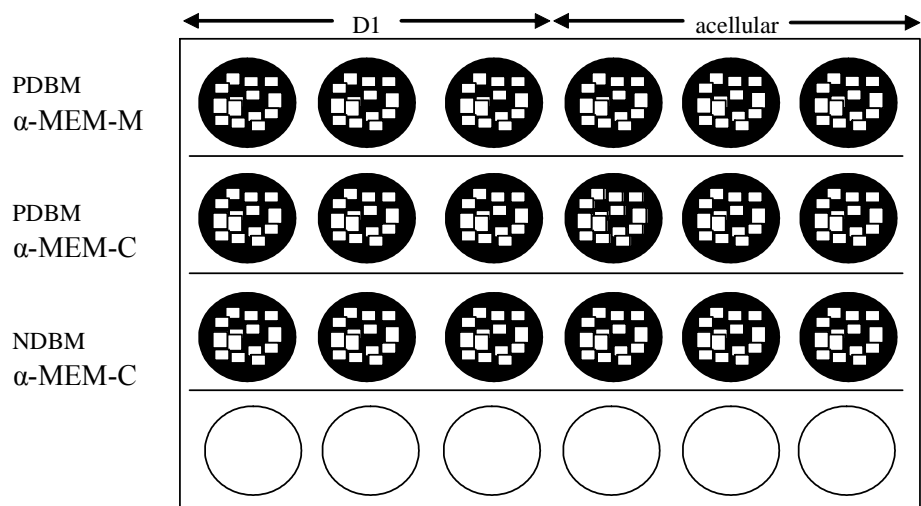
Cell Seeding

One day prior to cell seeding, the sterilized bone fragments underwent a conditioning process in sterile 50 mL centrifuge tubes to ensure that all residual HCl was removed. The fragments were washed twice in 10 minute intervals in sterile PBS (Sigma), then immediately rinsed five times (30 minutes per rinse), and then rinsed for 12-hours in α -MEM-C, as described previously.

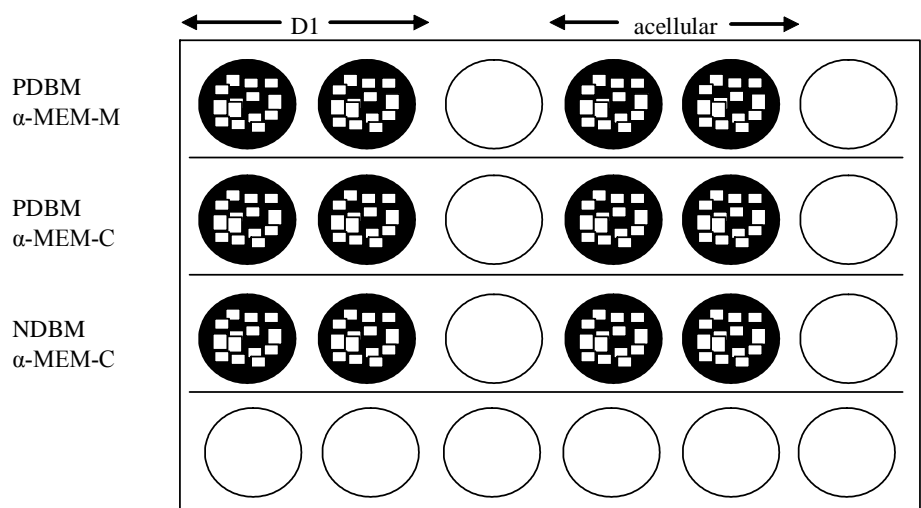
Fresh α -MEM-C was added to each set of bone fragments after the conditioning cycle was completed. The bone fragments were transferred in 0.1 mL quantities to well plates with modified EtO sterilized pipets, as portrayed in Figure 3. One mL of fresh α -

MEM-C was then added to each well. The well plates were placed in a sterile hood overnight. Four time points were selected and four plates for each time point were prepared, resulting in a total of 16 ultra-low attachment plates (Corning).

The spent media was aspirated from the well plates and replaced with 1 mL of α -MEM-M on the day of cell seeding, as shown in Figure 3. Multipotent mouse marrow stromal cells (D1's) (#CRL-12424, ATCC) of passage 32 were seeded into each well at a density of 3×10^5 cells/well. The negative acellular control group received bone fragments and medium, but no cells. All wells were placed in an incubator under standard conditions of 37°C and 5% CO₂ on an orbital shaker (IKA[®] Works) set in motion at approximately 50 rpm. The day of cell seeding was denoted as Day 0 of the study. The medium was changed on Days 2, 4, 6, 8, 10, 12, 13, 15, 16, 18, 20, 22, 24, 26, 28, 30, 32, 34, and 36 during the 36-day study.



1 plate/time point for gene expression
 1 plate/time point use for BCA, ALP, then calcium assays
 1 Day 24 plate used for lactic acid/glucose and Alamar Blue™ for all time points
 Total of 8 plates prepared with this layout



1 plate/time point for cell viability
 1 plate/time point for histology
 Total of 8 plates prepared with this layout


 α -MEM-M and bone fragments

Figure 3 Plate set-ups for the level of demineralization study

Qualitative Microscopy

Cell Viability

A LIVE/DEAD[®] Viability/Cytotoxicity kit (Molecular Probes, Eugene, OR) was used, as described earlier, to analyze the cells on the bone fragments and to determine if the medium conditions affected the viability of the cells on Days 4, 13, 24 and 36.

Histology

Samples for histological analysis were processed on Days 4, 13, 24, and 36. At the desired time point, each well in the specified plate was rinsed twice with sterile PBS (Sigma), and 1 mL of 10% neutral buffered formalin was added to each well. The plate was stored at 4°C for 24 hours. A Technovit 7100 GMA embedding kit (EBSciences, East Granby, Connecticut) was used to prepare and embed the bone samples. Samples were pre-infiltrated with increasing concentrations of GMA as listed in Table 5. Samples were then infiltrated for 24 hours with mild agitation at 22°C with Solution A, which consisted of a ratio of 100 mL of GMA monomer for every gram of Hardener I. Following infiltration, fragments were dried and placed into separate molds in a molding tray. An embedding solution consisting of 15 parts of Solution A and 1 part of Hardener II was mixed for one minute and immediately used to embed the bone fragments. Samples were stored in a dessicator at room temperature until sectioning. Eight micrometer sections were obtained using a RM2155 rotary microtome (Leica). Sections were stained with hemotoxylin and eosin (H&E), to study the cellular attachment on the

bone, and von Kossa, to analyze the mineralization of the bone. Protocols can be found in Appendices A and B. Images were captured using an Axiovert 135 microscope (Zeiss), a ProgResTM C10^{Plus} digital color camera and ProgRes Capture Basic 1.2 software (both from Jenoptik). The images were analyzed with Image-Pro Plus 5.1 Software (Media Cybernetics).

Table 5 Pre-infiltration series

Step	% of GMA monomer	Time	Temperature
1	5%	1 hour	Room
2	10%	1 hour	Room
3	20%	1 hour	Room
4	30%	1 hour	Room
5	40%	1 hour	Room
6	50%	1 hour	Room
7	60%	1 hour	Room
8	70%	1 hour	Room
9	80%	1 hour	Room
10	90%	1 hour	Room
11	100%	1 hour	Room

Real-Time Quantitative Testing

Metabolic Activity

Lactic Acid and Glucose Levels

The lactic acid and glucose levels were analyzed at every medium change, which occurred on Days 2, 4, 6, 8, 10, 12, 13, 15, 16, 18, 20, 22, 24, 26, 28, 30, 32, 34, and 36. Before the medium was aspirated, 400 μ L of spent medium was removed from each well and analyzed using a YSI 2700 SELECT™ biochemistry analyzer (YSI, Yellow Springs, OH). The YSI analyzer was used, as described previously, to analyze lactic acid and glucose levels in the medium.

Alamar Blue™

The metabolic activity of the cells seeded on the demineralized bone fragments was assessed on Days 4, 13, 24 and 36 using an Alamar Blue™ dye (BioSource International), as described previously. Briefly, after aliquots were removed for lactic acid and glucose monitoring, spent media was removed and replaced with 1 mL of α -MEM-M and incubated for 4 hours. The dye was added at this time and allowed to incubate for an additional 3 hours. Medium aliquots were transferred in triplicate to a clear 96-well plate (Corning). The fluorescence values were read on a SpectraMax® Gemini EM Dual scanning spectrofluorometer (Molecular Devices). The remaining medium in the 24-well plates was aspirated and replaced with 1 mL of fresh medium.

Post-Study Quantitative Testing

The 24-well plate specified for post-study quantitative testing at each time point was rinsed twice in sterile PBS (Sigma). Following the rinse, 1 mL of 0.5% Triton-X (Fisher Scientific) in PBS (Sigma) was added to lyse the cells. The plates were frozen at -80°C until the plates for all time points were collected. The plates underwent three freeze/thaw cycles to lyse and release the proteins. At this time, samples were removed for alkaline phosphatase and intracellular protein assays. The remaining cell lysate and bone fragments were used for the extracellular calcium assay.

Intracellular Protein

The intracellular protein content was determined using a BCA Protein Assay Reagent Kit (Pierce Biotechnology) and following manufacturer protocol. The assay was performed as previously described. This data was used to normalize results from alkaline phosphatase and extracellular calcium assays.

Alkaline Phosphatase

The alkaline phosphatase content of each sample was determined following manufacturer protocol from Kit #104 (Sigma). The ALP activity values were normalized using the total intracellular protein content.

Extracellular Calcium

The remaining bone fragments and cell lysates were used to determine the extracellular calcium content. Samples were prepared for analysis as previously described. After thawing the samples, PDBM samples were diluted 1:10 with the atomic absorption matrix solution and CDBM and NDBM samples were diluted 1:100 with the same solution. The matrix solution consisted of 0.3 *N* Ultrapure HCl and 0.5% (w/v) lanthanum oxide (Alfa Aesar, Ward Hill, MA). Samples were analyzed with a Perkin Elmer 3030 atomic absorption flame spectrophotometer (Perkin Elmer) as described previously. The total extracellular calcium was normalized with the intracellular protein content.

Gene Expression

The expression of osteoblast-specific genes was monitored by performing real-time reverse transcription-polymerase chain reaction (RT-PCR) on Days 4, 24, and 36. Ribonucleic acid (RNA) was isolated from the tissue culture and the quantity and quality of each sample was analyzed. Primers and reaction parameters were optimized before real-time RT-PCR testing was completed on all samples.

RNA Isolation

RNA was isolated from the culture on Days 4, 13, 24 and 36 by following manufacturer protocol and using an RNeasy[®] Mini Kit (Qiagen, Valencia, CA). The

fragments in the specified 24-well plate were rinsed twice in sterile PBS (Sigma). The cell membranes were lysed by the addition of 600 μ L of β -Mercapthoethanol (β - ME) (Sigma) and Buffer RLT solution. The lysis solution was composed of 10 μ L of β - ME per 1 mL of Buffer RLT. After remaining at room temperature for ten minutes, the samples were homogenized by placing the lysate from each sample onto a QIAshredder column placed in a 2 mL collection tube. The tubes were centrifuged for 2 minutes at 13,000 rpm. One volume (600 μ L) of 70% ethanol was added to the homogenized lysates in each tube. A volume of 700 μ L of the sample was deposited on an RNeasy mini column placed in a 2 mL collection tube and centrifuged for 15 seconds at 13,000 rpm. The flow-through was discarded before the remaining lysate (500 μ L) was placed into the same column and the centrifugation step was repeated. After discarding the flow-through, 350 μ L of Buffer RW1 was added to the RNeasy column, followed by centrifugation at 13,000 rpm for 15 seconds. DNase treatment was performed on the column using an RNase-free DNase Set (Qiagen), after discarding the flow-through from the first wash step with Buffer RW1. Eighty microliters of the DNase treatment (70 μ L of RDD buffer and 10 μ L of DNase I stock solution) was placed on the columns and remained on the bench top for 15 minutes. Another 350 μ L of Buffer RW1 was added to the RNeasy column, followed by centrifugation at 13,000 rpm for 15 seconds. RNA isolation continued as the flow-through and collection tubes were discarded. The RNeasy column was transferred to a new 2 mL collection tube and 500 μ L of Buffer RPE was added to the column. The tubes were centrifuged for 15 seconds at 13,000 rpm to wash the columns and the flow-through was discarded. An additional 500 μ L of Buffer RPE

was added to the column and each sample was centrifuged for 2 minutes at 13,000 rpm to dry the silica-gel membrane in the column. The columns were transferred to new 1.5 mL collection tubes in order to collect the RNA from the column. The first elution step was performed by adding 50 μ L of RNase free water to the column and centrifuging the column for one minute at 13,000 rpm. The elution step was repeated so that 100 μ L of RNA sample was collected for each replicate and fragment type from the cell culture. All samples were stored at -80°C immediately after the elution phase.

RNA Analysis

The purity and concentration of each RNA sample was determined using an RNA 6000 Nano Assay Kit (Agilent Technologies, Palo Alto, CA) and following the manufacturer protocol. Twelve RNA samples were tested at a time. The RNA samples and the RNA 6000 ladder (Agilent Technologies) were thawed on ice, while the remainder of the reagents were thawed at room temperature for 30 minutes. A gel mix was prepared by placing 550 μ L of RNA 6000 Nano gel matrix onto a spin filter and centrifuging it for 10 minutes at 4000 rpm. The gel was then aliquoted into tubes in 65 μ L quantities. A gel-dye mix was made by adding 1 μ L of RNA 6000 Nano dye concentrate to 65 μ L of gel. The tube was centrifuged for 10 minutes at 14,000 rpm. A RNA Nano chip was placed onto the Chip Priming Station and 9 μ L of the gel dye matrix was pipetted into a specific well on the chip. The gel-dye mix was distributed throughout the LabChip[®] by pressurizing it for 30 seconds using a Chip Priming Station. Nine μ L of the gel-dye mix was then added to two specific wells on the chip. The RNA 6000 Nano

Marker was added by pipetting 5 μL of the reagent into each of the 12 sample wells and a ladder well. A volume of 2 μL of the ladder was heat denatured for 2 minutes at 70°C before 1 μL of the ladder was added to the well marked ladder. RNA samples were added to each well in 1 μL quantities. The LabChip[®] was then vortexed for 1 minute at 2400 rpm and immediately placed in an Agilent 2100 Bioanalyzer (Agilent Technologies). Using Agilent 2100 Expert Software (Agilent Technologies), the Eukaryote Total RNA Nano program was used to calculate the RNA concentration and purity of each sample. This analysis was repeated for all RNA samples. All samples were placed back at -80°C until real-time RT-PCR was performed.

Primer Design

Three genes were selected to monitor the differentiation of the mouse stromal cells to the osteoblast lineage: runt-related transcription factor 2 (Runx2), bone sialoprotein (BSP), and osteocalcin (OCN). The gene β -actin was used as the housekeeping gene. Runx2 regulates extracellular bone matrix gene expression including osteocalcin, bone sialoprotein, osteopontin, and type I collagen [54, 55]. Therefore, Runx2 is expressed in pre-osteoblasts [13]. BSP is restricted to cells that have secreted and are actively mineralizing type I collagen; therefore, it is only expressed in newly formed mineralizing osteoblasts [13]. OCN is synthesized by osteoblasts and is considered a late marker for differentiation of cells into osteoblasts.

Target primers were designed using the method presented in Appendix C. The selected primers (Table 6) were ordered from Integrated DNA Technologies (IDT,

Coralville, IA), and were received in a lyophilized powder form. The primers were resuspended in RNase-free water at a concentration of 100 μ M, aliquoted into 1.5 mL nuclease-free tubes and stored at -20°C.

Table 6 Primers for real-time RT-PCR

Target Gene	Accession Number	Forward primer (5'-3')	Reverse Primer (5'-3')	Amplicon Size (bp)
β -actin	NM007393	CCCTGAACCCCTAAGGCCAAC	GCATACAGGGACAGCACAGC	105
Runx2	AF10284	GACTTCTGCCCTCTGGCC TTC	GGTAGTGCATTTCGTGGGTTG	142
Bone Sialoprotein	BC045143	TACGGAGCAGAGACCACACC	CTTCTTCTCGTCGGCTTTCC	121
Osteocalcin	BC101948	CCAAGCAGGAGGGCAATAAG	GTCACAAGCAGGGTCAAGCTC	119

Real-Time RT-PCR

A QuantiTect[®] SYBR[®] Green RT-PCR Kit (QIAGEN) was used to determine the relative gene expression levels in the RNA samples. The manufacturer's protocol was followed for performing the real-time RT-PCR reactions on a Rotor-Gene[™] RG-3000 centrifugal thermal cycler (Corbett Research, Australia) using a 36 well rotor. The QuantiTect[®] RT-PCR Master Mix, RNase-free water, primers, and RNA samples were thawed on ice and then combined with the QuantiTect[®] RT Mix (Figure 6). Stock primer solutions were diluted to concentrations of 20 μ M by the addition of RNase-free water and added to the PCR solutions so that the final concentration of primer in each reaction was 0.4 μ M. The reaction components were pipetted in specific volumes into 0.2 mL RT-PCR reaction tubes (Fisher Scientific) on ice (Figure 7). Non-template control solutions were prepared without RNA samples and –RT control solutions were made without the QuantiTect[®] RT Mix. RNA samples were diluted either 1:2 or 1:4 with RNase-free water to provide a 20 ng sample of RNA so that a volume of RNA greater than 0.8 μ L was added for each reaction. RNase-free water was added all PCR reaction tubes to bring the final reaction volume to 50 μ L. The cycler was set up as indicated in the QuantiTect[®] SYBR[®] Green RT-PCR Kit manufacturer handbook and included a reverse transcription step, an activation step, and either 35 or 40 four-step cycles (35 was suitable for most reactions but one set of data needed a 40 step cycle) that included denaturation, annealing, and extension (Table 8).

Table 7 Real-time RT-PCR reaction components

Reagent	Volume per reaction (μL)	Final concentration
QuantiTect [®] RT-PCR Master Mix	25	1x
QuantiTect [®] RT-Mix	0.5	0.5 μL /reaction
Forward primer	1	0.4 μM
Reverse primer	1	0.4 μM
Template RNA	Variable	20 ng/reaction
RNase-free water	Variable	--

Table 8 Real-time RT-PCR cycler conditions

Step	Time	Temperature
Reverse Transcription	30 minutes	50°C
PCR Initial Activation	15 minutes	95°C
4-Step Cycle (x 35)		
Denaturation	15 seconds	94°C
Annealing	30 seconds	50°C
Extension #1	30 seconds	72°C
Extension #2	15 seconds	75°C

The cycle number in the exponential phase of amplification at a specific threshold, C_T , was recorded for each sample reaction.

Amplification Efficiency Determination

The comparative C_T analysis method is only valid if the difference between the amplification efficiency of the sample amplification and the efficiency amplification of β-actin is less than 5%. To determine if this method was viable for the data set, real-time RT-PCR reactions were performed in triplicate for each target gene using the following serial dilution series: 20 ng, 2.0 ng, and 0.2 ng. The reactions were prepared and carried out as described previously. RNA from a Day 36 CDBM sample was used for this analysis. Average C_T values for each target gene were plotted versus LOG₁₀ of the RNA quantity. Linear regression was performed on each target gene graph separately and the amplification efficiency was determined by:

$$E=10^{(-1/\text{slope})} - 1 \quad (7.1)$$

Statistical Analysis

All quantitative assays were executed in triplicate. Statistical analysis was performed using SAS[®] System 9.1 statistical software (SAS Institute Inc.). The Least Squares Mean (LSMEANS) method was used to determine the effects of the level of demineralization on the cellular activity over time of cells seeded on DBM in all quantitative assays. Values are represented by a standard error of mean (SEM) for a sample number, n, of 3. A significance level of p = 0.05 was employed for all comparisons.

RESULTS

Evaluation of Media Cocktails

Bone Matrix Preparation

Stereomicroscope digital images of bone fragments were acquired after each forty minute HCl demineralization cycle (Figure 4).

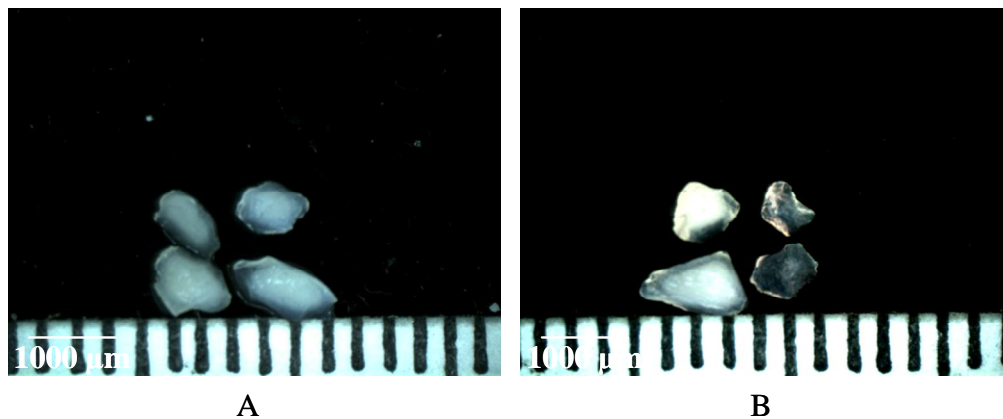


Figure 4 Stereomicroscope images
Images obtained of bone fragments that were demineralized for 80 minutes.

The bone fragments had bright areas of mineralization even after 80 minutes of demineralization. Demineralized regions surrounding the mineralized areas appeared glassy. As a result, PDBM fragments were acquired after 80 minutes of demineralization in the 0.5 *N* HCL.

Cell Seeding

During the conditioning process, the medium immediately turned orange following the first bone fragment wash and gradually changed to yellow as the thirty minutes progressed. By the end of the last step of the conditioning sequence, the medium remained pink, indicating that no residual acid remained on the bone fragments.

Qualitative Microscopy

Cell Viability

Representative fluorescence micrographs display the viability of D1 cells on the demineralized bone fragments (Figure 5). The fragments in each image have irregular shapes and vary in size. The cells attached to the DBM fragments in all culture conditions by Day 4 of the study (Figure 5). A larger number of live cells were visible on the DBM fragments in the medium containing osteogenic supplements (OSTEO) on Day 13 than on the DBM fragments in the other conditions. It appeared that the number of cells on the DBM in the medium without osteogenic supplements (NOSTEO) and on the negative control fragments decreased between Day 13 and Day 4. The number of viable cells appeared to decrease in all media by Day 24 of the study. As time increased, it seemed that the number of dead cells remaining on the bone fragments increased. The ratio of live cells to dead cells was large at all time points for all three conditions.

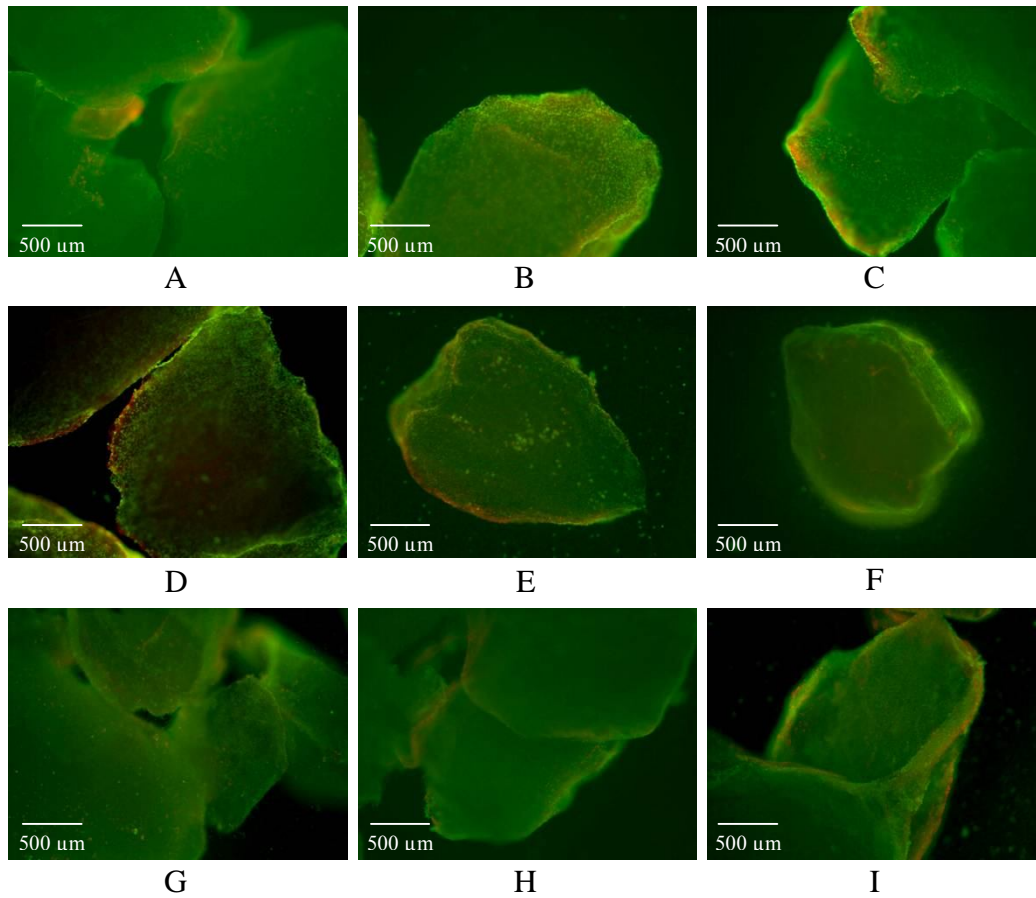


Figure 5 Cell viability

Fluorescence micrographs demonstrating cellular attachment and coverage of D1 cells for three media and DBM conditions.

- | | | |
|------------------|-------------------|--------------------|
| (A) OSTEO Day 4 | (B) NOSTEO Day 4 | (C) CONTROL Day 4 |
| (D) OSTEO Day 13 | (E) NOSTEO Day 13 | (F) CONTROL Day 13 |
| (G) OSTEO Day 24 | (H) NOSTEO Day 24 | (I) CONTROL Day 24 |

Histology

H&E staining was performed to illustrate cell distribution on the DBM fragments and von Kossa staining was performed to assess mineralized areas of the bone fragments. Light micrographs portray the staining results (Figure 6-7). Light micrographs of the samples stained with H&E showed cellular attachment on the surface of bone fragments from all three conditions. The images displayed in Figure 6 are representative of images obtained for each specific condition at the specified time point. On Day 4, multiple layers of cells were attached to the outer surface of the NOSTEO fragments and a single layer of cells attached to fragments cultured in osteogenic supplemented media and the control fragments. The number of cell layers was uniform for the control and the fragments cultured in osteogenic supplements on Day 4, while the number of layers on the surface of NOSTEO fragments varied greatly between samples. Cellular infiltration was evident on Day 4 for both sample DBM fragments. Results from the H&E staining did not suggest that the configuration and quantity of cells on OSTEO fragments was significantly different from the configuration and quantity on NOSTEO fragments between Days 4 and 13. Cellular infiltration was evident on the control fragments on Day 13. The thickest layers of cells attached to the bone surface and the greatest degree of cellular infiltration into the bone for all cultures was observed on Day 24.

Light microscopy of PDBM fragments revealed mineralized portions of the tissue (Figure 7). Day 4 fragments cultured with osteogenic supplements consistently contained centrally located mineralized areas. Day 4 NOSTEO and control fragments contained variable amounts of mineralization. Most of the control fragments, and the fragments

cultured in non-osteogenic supplemented media, contained only small areas of mineralization, dispersed throughout the sample, although a small number of fragments did contain larger, centrally located mineralized areas. Experimental samples from Day 13 contained regions of mineralization dispersed through the tissue sample, but these areas were smaller than the mineralized areas observed on Day 4 in the OSTEO fragments. Select Day 13 OSTEO fragments contained larger areas of mineralized tissue in the center of the bone, while many of the fragments still contained only smaller areas of mineralization. The number of cells on the surface of the PDBM fragments cultured in osteogenic supplemented media (OSTEO) containing large mineralized regions was greater than on the OSTEO fragments containing only small mineralized areas on Day 13. Fragments cultured in media without osteogenic supplements (NOSTEO) showed good cellular infiltration but minimal mineralized areas on Day 24. PDBM control fragments contained areas of mineralization on the edges, with only small areas within the fragment on Day 24. Day 24 OSTEO fragments were similar to Day 4 fragments, except the Day 24 samples also contained select, small mineralized areas.

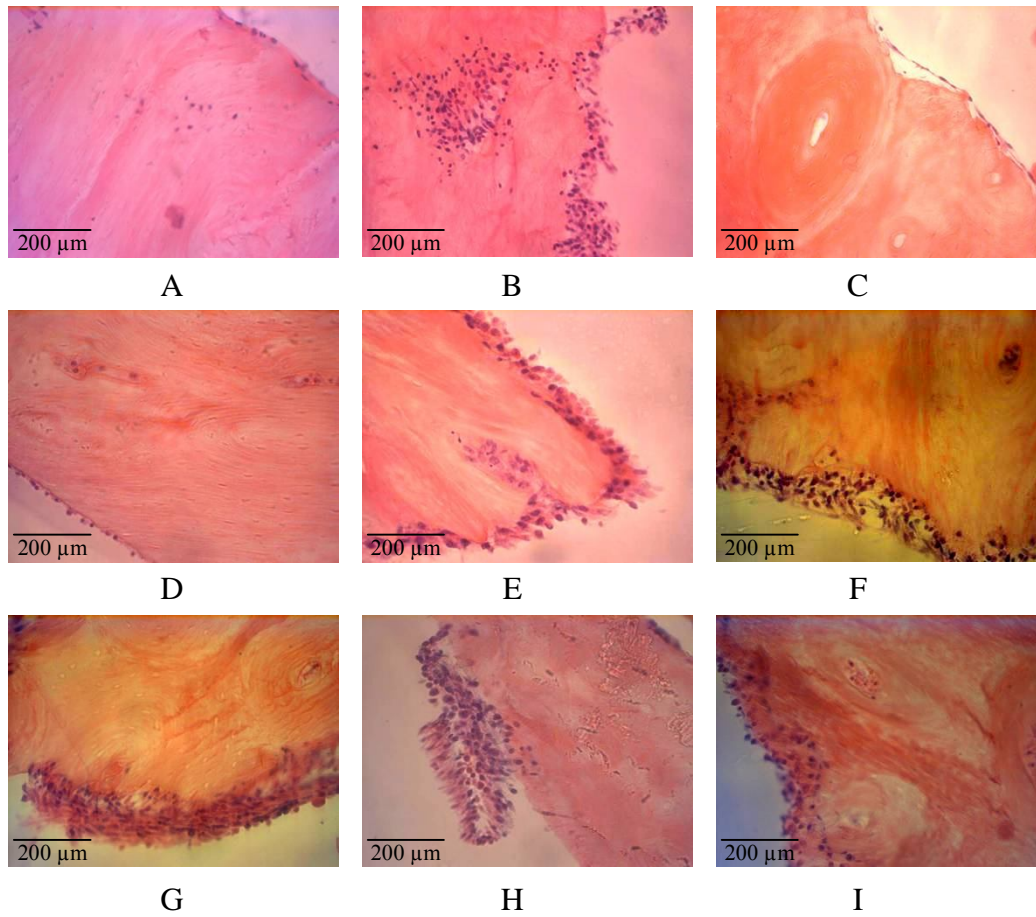


Figure 6 H&E light micrographs

Light micrographs showing attachment and distribution of D1 cells. Images obtained after H&E staining.

Pink: DBM Dark purple: nuclei Light purple: cytoplasm, extracellular matrix.

- | | | |
|------------------|-------------------|--------------------|
| (A) OSTEO Day 4 | (B) NOSTEO Day 4 | (C) CONTROL Day 4 |
| (D) OSTEO Day 13 | (E) NOSTEO Day 13 | (F) CONTROL Day 13 |
| (G) OSTEO Day 24 | (H) NOSTEO Day 24 | (I) CONTROL Day 24 |

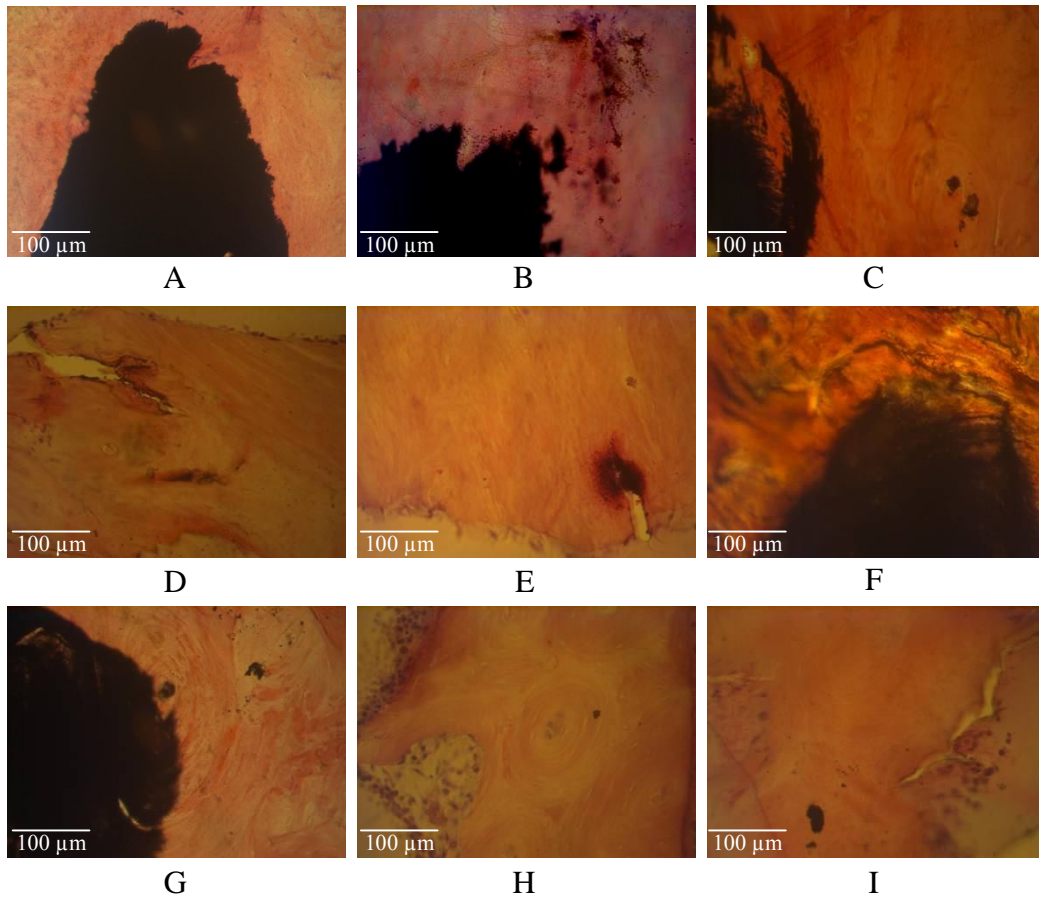


Figure 7 von Kossa light micrographs

Light micrographs obtained after von Kossa staining with eosin counterstain.

Light pink: DBM	Dark pink: cells	Black: mineralized matrix
(A) OSTEO Day 4	(B) NOSTEO Day 4	(C) CONTROL Day 4
(D) OSTEO Day 13	(E) NOSTEO Day 13	(F) CONTROL Day 13
(G) OSTEO Day 24	(H) NOSTEO Day 24	(I) CONTROL Day 24

Real-Time Quantitative Testing

Metabolic Activity

Lactic Acid and Glucose Levels

The cumulative lactic acid production for each media condition increased over time (Figure 8). The level of lactic acid production of OSTEO fragments (cultured in osteogenic supplemented media) on Days 4 and 24 was significantly higher ($p < 0.05$) than that of the negative control cultures and significantly higher ($p < 0.05$) than that in NOSTEO fragments (cultured in media lacking osteogenic supplements) cultures on Days 13 and 24.

The total glucose consumption increased over time for each medium and fragment condition (Figure 9). The PDBM with osteogenic supplemented medium (OSTEO) had significantly lower ($p < 0.05$) levels of total glucose than the negative control on Days 4, 13, and 24. A significant difference in total glucose consumption was not observed between OSTEO and NOSTEO cellular cultures or NOSTEO and control cellular cultures at any time point.

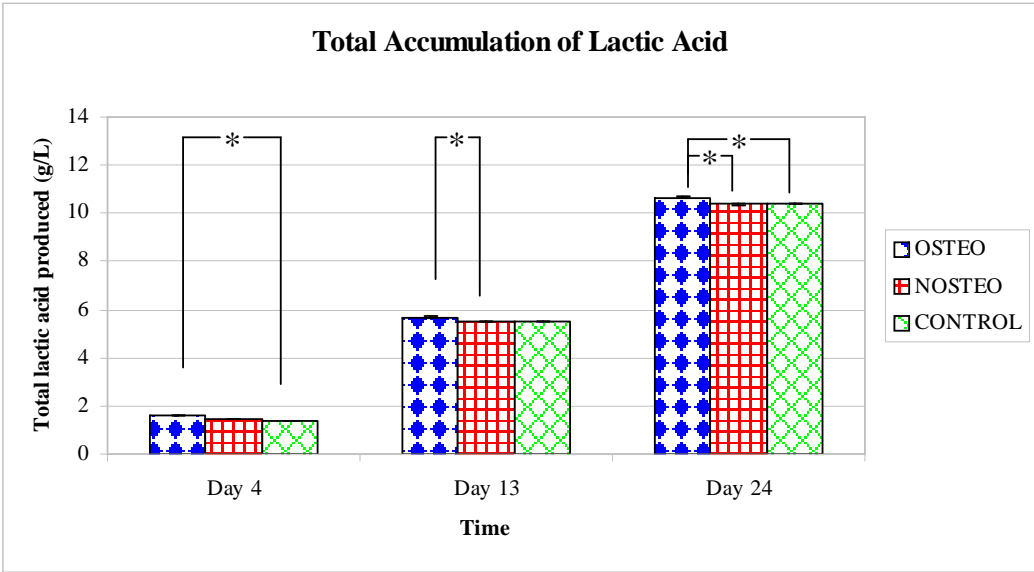


Figure 8 Cumulative lactic acid production
 Total lactic acid production as a function of culture day. Each data point represents the mean of three values, and error bars denote SEM. Asterisks denote statistical differences ($p < 0.05$) in lactic acid levels with respect to time.

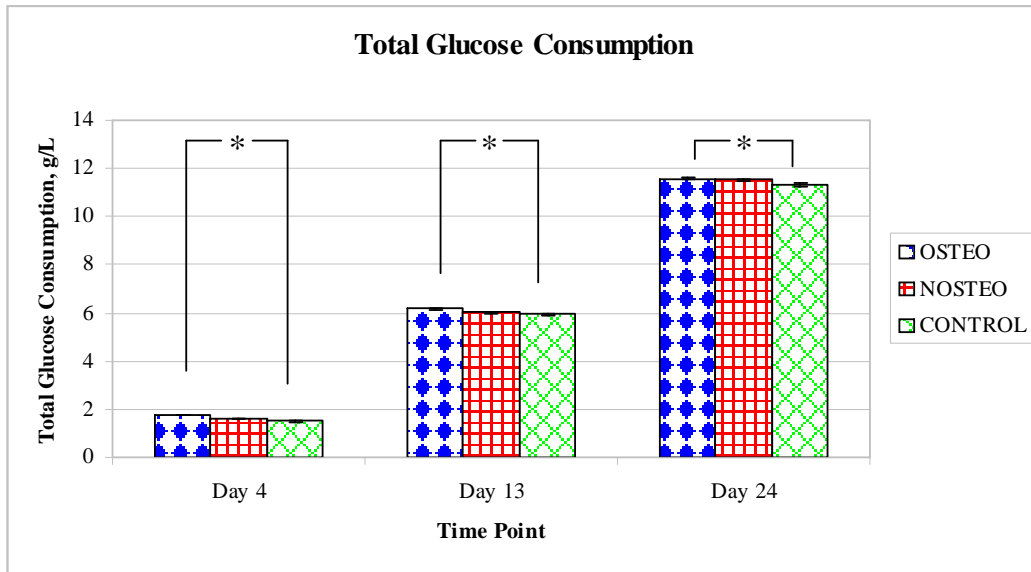


Figure 9 Cumulative glucose consumption
 Cumulative glucose consumption as a function of culture day. Each data point represents the mean of three values, and error bars denote SEM. Asterisks denote statistical differences ($p < 0.05$) in glucose level with respect to time.

Alamar Blue[™]

The Alamar Blue[™] assay results indicated that the metabolic activity was not significantly different between the two experimental PDBM mediums on Days 4 and 13 (Figure 10). On Day 24, the medium containing no osteogenic supplements (NOSTEO) had a significantly higher ($p < 0.05$) metabolic activity level than the medium containing the osteogenic supplements (OSTEO). The metabolic activity of the control samples on Day 13 was significantly larger ($p < 0.05$) than the medium without osteogenic supplements. No significant differences existed on Day 4 between any of the cultures.

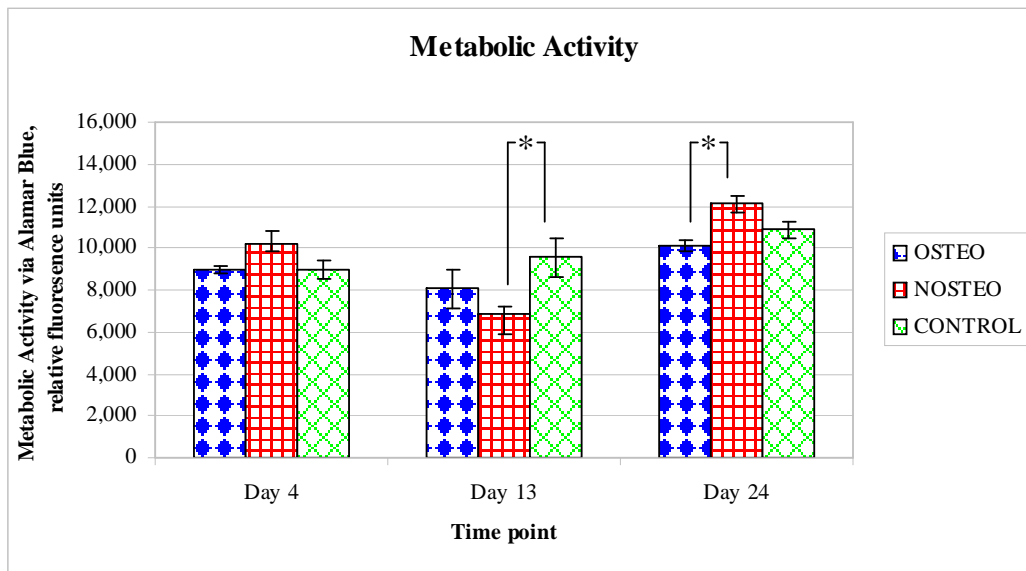


Figure 10 Metabolic activity via Alamar Blue™
 Metabolic activity as a function of culture day for each fragment type. Each data point represents the mean of three values, and error bars denote SEM. Asterisks denotes statistical differences ($p < 0.05$) in metabolic activity with respect to time.

Post-Study Quantitative Testing

Intracellular Protein

No significant differences in the protein levels were detected between the medium conditions at each time point observed (Figure 11). A single condition did not have a significantly higher level of intracellular protein content ($p < 0.05$) at any of the three time points. The intracellular protein contents on the control and the fragments cultured in osteogenic supplemented media increased from Day 4 to Day 13, then decreased on

Day 24. The protein levels measured in the NOSTEO (no osteogenic supplements) systems increased over the observed time period.

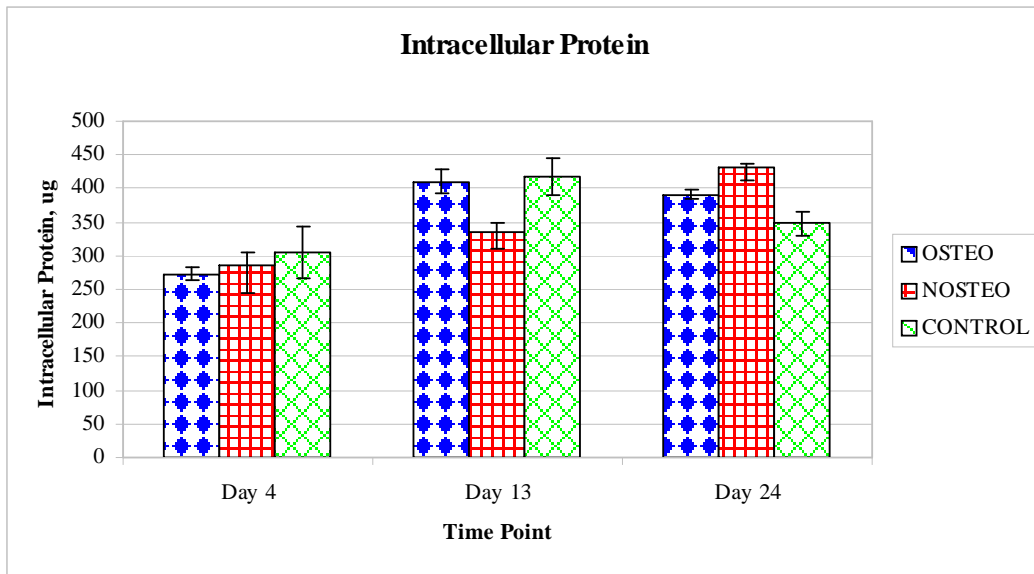


Figure 11 Intracellular Protein

Intracellular protein level as a function of time for each fragment type. Each data point represents the mean of three values, and error bars denote SEM. Asterisks denote a statistical difference ($p < 0.05$) in intracellular protein level with respect to time.

Alkaline Phosphatase

Overall, the ALP activity in the three cultures increased between Days 4 and 24, although the activity decreased between Days 4 and 13 for the medium with osteogenic supplements, before increasing on Day 24 (Figure 12). The medium containing osteogenic supplements (OSTEO) had significantly lower ALP levels on Day 24 than

both the negative control and the samples cultured in the medium without osteogenic supplements (NOSTEO). OSTEO cultures had the highest level of ALP activity on Day 4, but then had the lowest levels on Days 13 and 24. Control fragments had the highest ALP activity levels on Days 13 and 24.

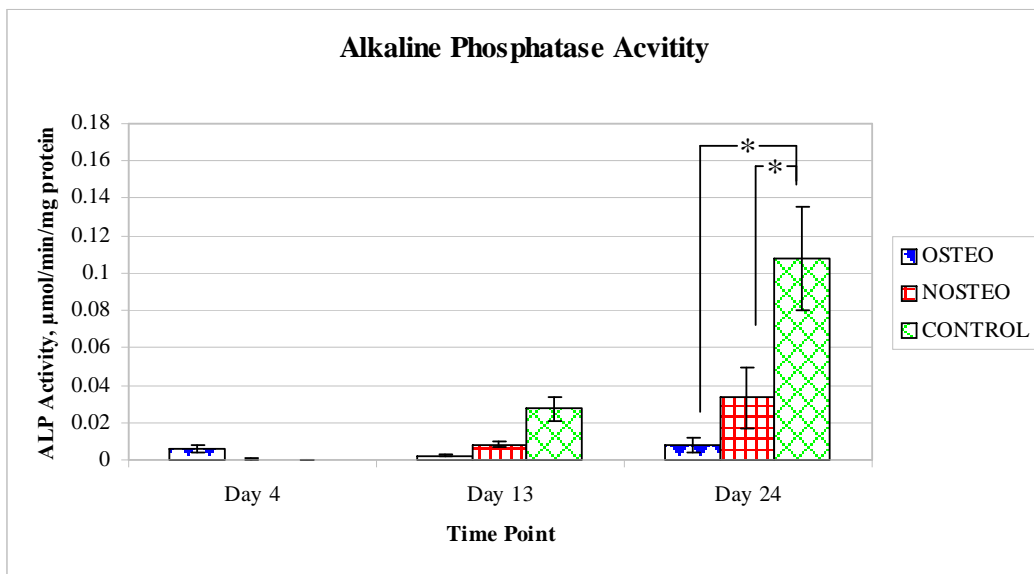


Figure 12 Alkaline phosphatase activity
ALP levels as a function of time for each fragment type. Each data point represents the mean of three values, and error bars denote SEM.

*Asterisks denote a statistical difference ($p < 0.05$) in ALP level with respect to time.

Extracellular Calcium

The level of extracellular calcium observed on Day 4 in the negative control cultures was significantly higher ($p < 0.05$) than the level observed in the cultures with

medium containing osteogenic supplements (OSTEO) (Figure 13). The extracellular calcium content of the OSTEO cultures increased over the course of the study. The highest level of observed extracellular content in both the NOSTEO and control cultures occurred on Day 4 of the study. Both these conditions decreased on Day 13 and then increased on Day 24. The observed extracellular calcium levels from the control and the samples cultured without osteogenic supplements were lower on Day 24 than the initial levels observed on Day 4.

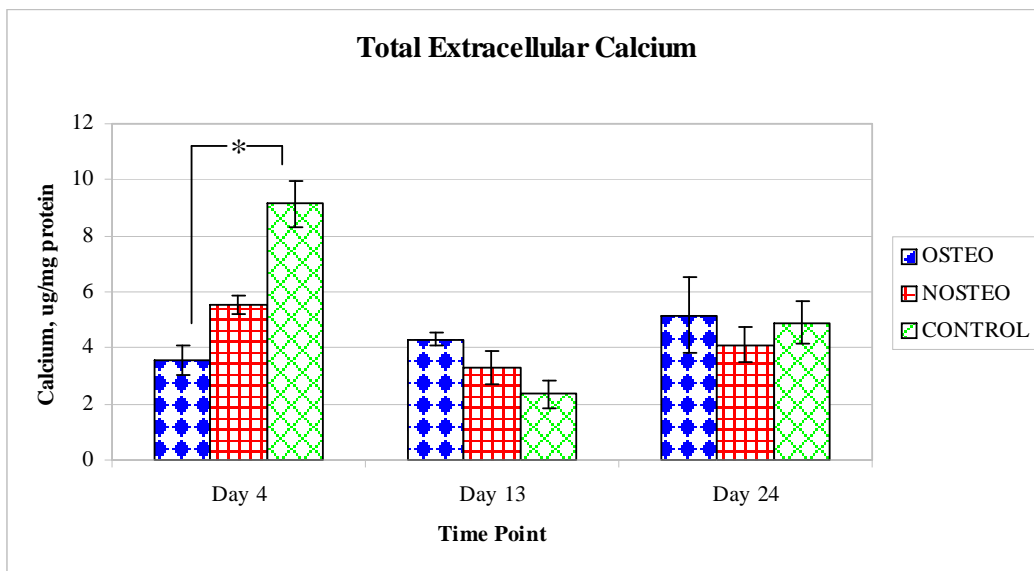


Figure 13 Extracellular calcium

Extracellular calcium levels as a function of time for each fragment type. Each data point represents the mean of three values, and error bars denote SEM.

Asterisks denote statistical differences ($p < 0.05$) in extracellular calcium level with respect to time.

In Vitro Evaluation of DBM

Bone Matrix Preparation

Stereomicroscopic digital images were acquired of bone fragments (Figure 14) after each forty minute HCl cycle in order to determine the demineralization endpoint for each sample group. The cumulative time of demineralization is displayed with each image.

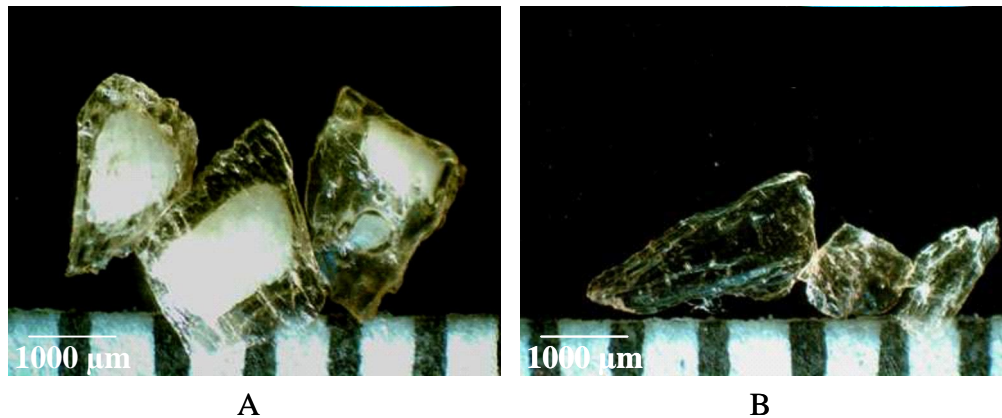


Figure 14 Stereomicroscope images of bone fragments
A) shows PDBM fragments after 80 minutes of demineralization. (B) CDBM fragments after 200 minutes of demineralization.

Bright areas within the bone fragments in the stereomicroscope images signify mineralized areas of the bone. Examination of bone fragments after 80 minutes, revealed mineralized cores with outer, mineralized regions. These fragments were considered to be partially demineralized and thus fragments were removed at this time and denoted

PDBM. Mineralization was not evident after 200 minutes of demineralization. Thus, CDBM fragments were collected at this time. The fragments displayed in Figure 14 are representative of fragments obtained for each time point.

Cell Seeding

The media color was monitored during the conditioning process to ensure any residual acid was removed from the bone before cell seeding. After the addition of the medium to the bone fragments for the first wash, the medium changed from red to orange to yellow over the course of the thirty minutes. By the end of the last step of the conditioning sequence, the medium remained pink, indicating that no residual acid remained on the bone fragments.

Qualitative Microscopy

Cell Viability

Fluorescence micrographs obtained after cytotoxicity testing demonstrate the viability of D1 cells on the demineralized bone fragments (Figure 15). The micrographs display select bone fragment size and shape irregularity; however, overall the fragments were similar in size and shape. The fragments displayed in Figure 15 are representative of fragments photographed in the micrographs obtained from other fragments within each sample as well as each replicate for each fragment type.

Cells readily attached to the PDBM and CDBM fragments by Day 4 of the study, and did not attach to the bottom of the wells, as noted by the green fluorescence seen in Figure 15. Cells attached to the NDBM at this time point but did not appear confluent until Day 13. Dead cells were visible on Day 13 for all fragment conditions, as noted by the red fluorescence on the bone fragments. The number of visible dead cells increased over time for each fragment condition. Few cells remained on the NDBM by Day 36. The surfaces of the bone fragments appeared to be fully covered on Day 4, Day 13, Day 24, and Day 36.

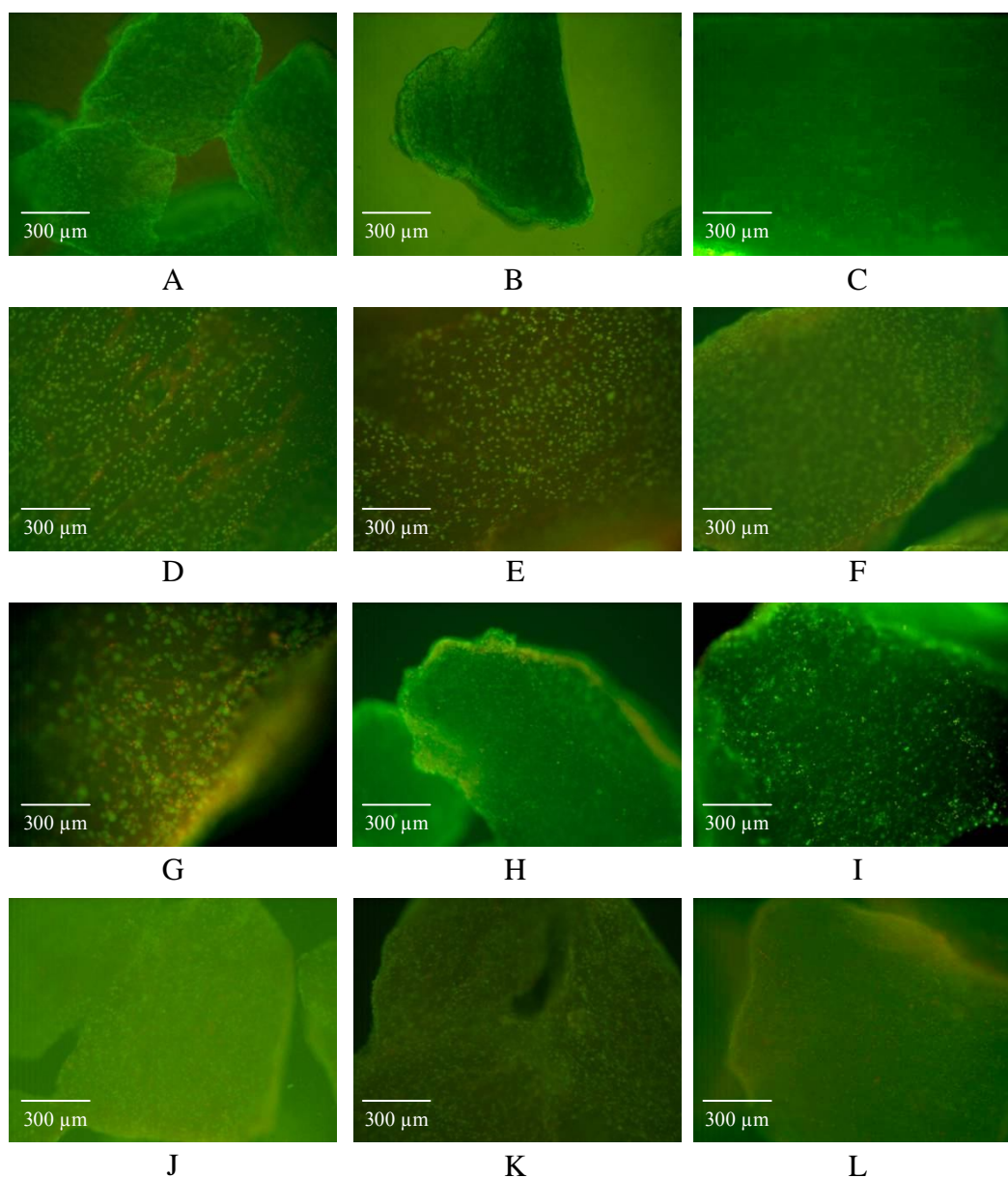


Figure 15 Cell viability
 Fluorescence micrographs demonstrating cellular attachment and coverage of three media and DBM conditions.

Images obtained following LIVE/DEAD[®] Viability assay.

- | | | |
|-----------------|-----------------|-----------------|
| (A) PDBM Day 4 | (B) CDBM Day 4 | (C) NDBM Day 4 |
| (D) PDBM Day 13 | (E) CDBM Day 13 | (F) NDBM Day 13 |
| (G) PDBM Day 24 | (H) CDBM Day 24 | (I) NDBM Day 24 |
| (J) PDBM Day 36 | (K) CDBM Day 36 | (L) NDBM Day 36 |

Histology

H&E staining was performed to illustrate cell distribution on the DBM fragments and von Kossa staining was performed to demonstrate mineralization of the DBM fragments at each time point. Light micrographs portray the staining results for each type of stain on the bone fragments (Figure 16-17). Images displayed are representative of the fragments observed for each time point and fragment type.

H&E staining of Day 4 PDBM fragments portray a thin layer of cells attached to the surface of the bone fragments. As time increased, the number of cells attached to the outside of the PDBM increased. The level of cellular infiltration also increased over time. The cells were most abundant on the outside and within the PDBM fragments on Day 36. CDBM fragments had varying layers of cells on the outside of the bone fragments on Day 4 and 13 with more consistent layers of cells present on Days 24 and 36. Cellular infiltration was observed on CDBM fragments on Days 24 and 36. The least amount of cells was observed on and within the CDBM fragments on Days 4 and 13 while the most abundant number of cells was observed on Days 24 and 36. The layer of cells on the outside of NDBM fragments was similar to the layers found on Day 4 PDBM fragments and Day 13 CDBM fragments. Cellular infiltration of the NDBM fragments was observed on Day 13 and an increase of cellular infiltration was observed on each subsequent time point. Cellular infiltration was not as abundant within NDBM fragments as it was with PDBM and CDBM fragments over the course of the study. The cellular infiltration within PDBM fragments on Day 24 was similar to the cellular infiltration of CDBM fragments on Day 36.

On Days 4, 13, and 24, a thicker layer of cells existed on the surface of CDBM fragments than PDBM and NDBM fragments. Day 4 PDBM fragments had cellular infiltration while CDBM and NDBM fragments did not. Overall, the thickest layer of cells and the greatest amount of infiltration existed on the outside of PDBM fragments on Day 36. NDBM fragments and Day 4 PDBM fragments had the thinnest layers of cells during the study. NDBM fragments contained the least amount of infiltration at all time points observed in this study.

Von Kossa staining of Day 4 samples revealed that almost all PDBM fragments had similar, large mineralized centers. The mineralized areas appeared as circular regions with smooth edges. The fragments without a solid center had numerous mineralized areas. Day 13 images of PDBM were similar to those on Day 4. Small, black specks were visible surrounding the mineralized core on Day 24, indicating the presence of small mineralized areas outside the large mineralized center. The mineralized cores appeared to have irregular edges by Day 36. Small areas of black within the tissue were also visible. Most of the CDBM fragments on Day 4, observed after von Kossa staining, lacked mineralized areas of bone. A few of the CDBM fragments had spots of mineralization indicating that not all of the fragments were completely demineralized before cell culture was started. Day 13 CDBM fragments were unchanged in appearance from Day 4. By Day 24, slightly larger areas of mineralized bone were visible than at previous time points. CDBM images obtained on Day 36 were similar to images obtained on Day 24. Day 4 NDBM fragments were mainly void of mineralized centers, where only a few fragments had small areas of mineralized tissue.

Day 13 NDBM von Kossa images were largely similar to those taken at Day 4; however, Day 24 and Day 36 images had a small number of tissue areas with mineralized spots.

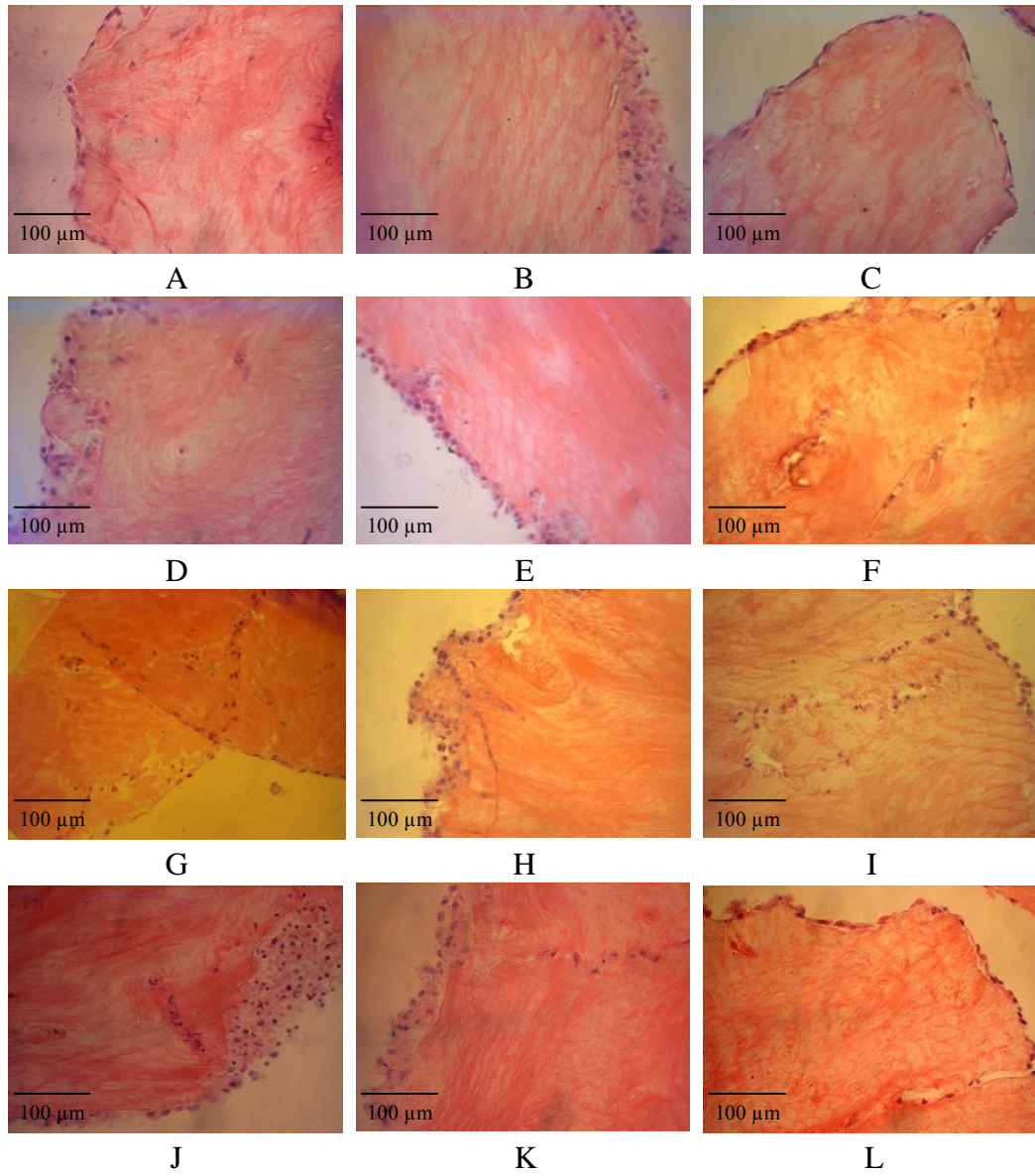


Figure 16 H&E light micrographs

Light micrographs obtained after H&E staining.

Pink: DBM Dark purple: nuclei Light purple: cytoplasm, extracellular matrix.

- | | | |
|-----------------|-----------------|-----------------|
| (A) PDBM Day 4 | (B) CDBM Day 4 | (C) NDBM Day 4 |
| (D) PDBM Day 13 | (E) CDBM Day 13 | (F) NDBM Day 13 |
| (G) PDBM Day 24 | (H) CDBM Day 24 | (I) NDBM Day 24 |
| (J) PDBM Day 36 | (K) CDBM Day 36 | (L) NDBM Day 36 |

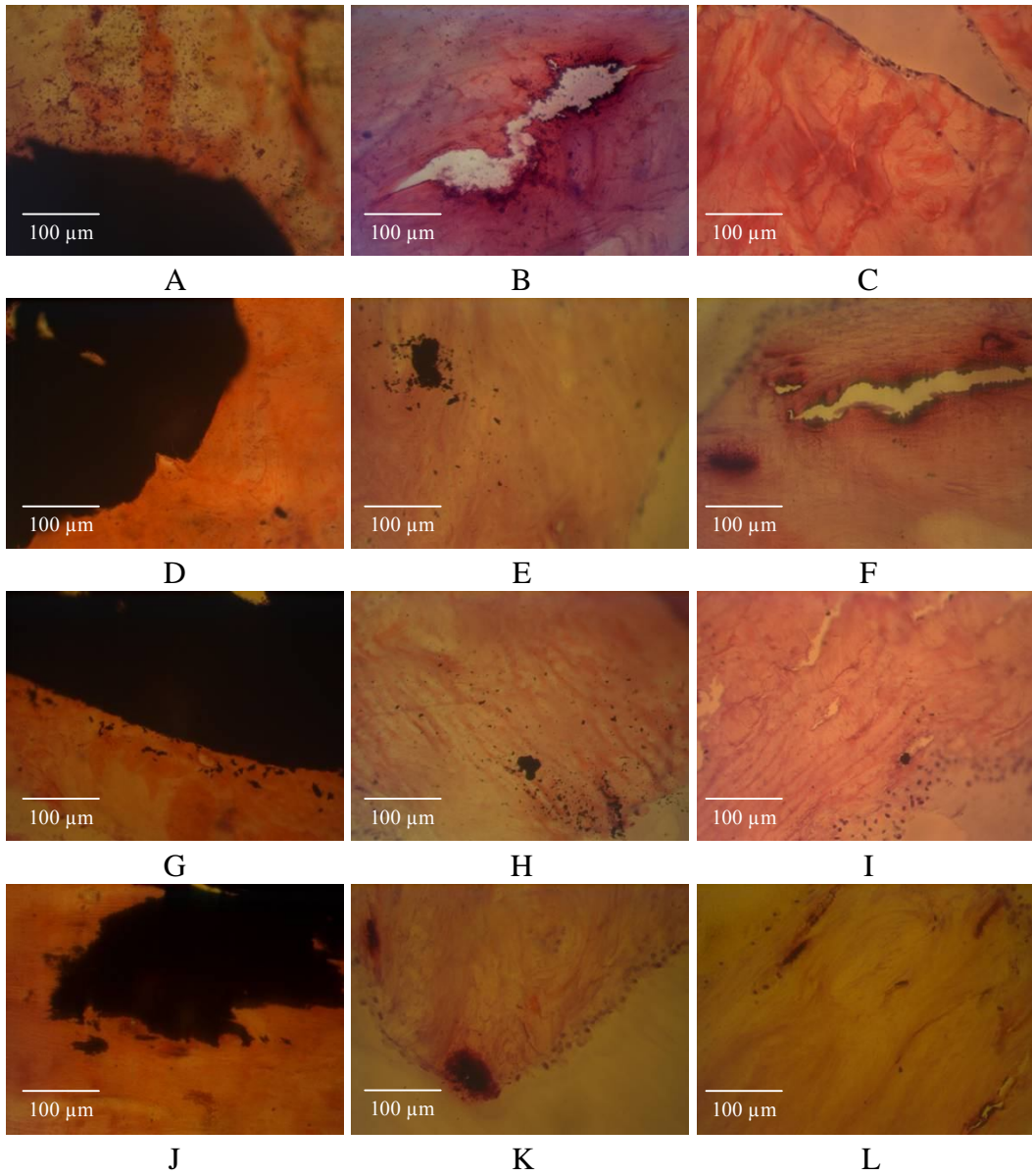


Figure 17 Von Kossa light micrographs

Light micrographs obtained after von Kossa staining with eosin counterstain.

Light pink: DBM Dark pink: cells Black: mineralized matrix

(A) PDBM Day 4

(B) CDBM Day 4

(C) NDBM Day 4

(D) PDBM Day 13

(E) CDBM Day 13

(F) NDBM Day 13

(G) PDBM Day 24

(H) CDBM Day 24

(I) NDBM Day 24

(J) PDBM Day 36

(K) CDBM Day 36

(L) NDBM Day 36

Real-Time Quantitative Testing

Metabolic Activity

Lactic Acid and Glucose Levels

The cumulative lactic acid production increased over time with respect to each fragment type. The level of total lactic acid accumulation for each fragment type increased significantly ($p < 0.05$) with time. The accumulation of lactic acid for each fragment type at each time point is displayed in Figure 18.

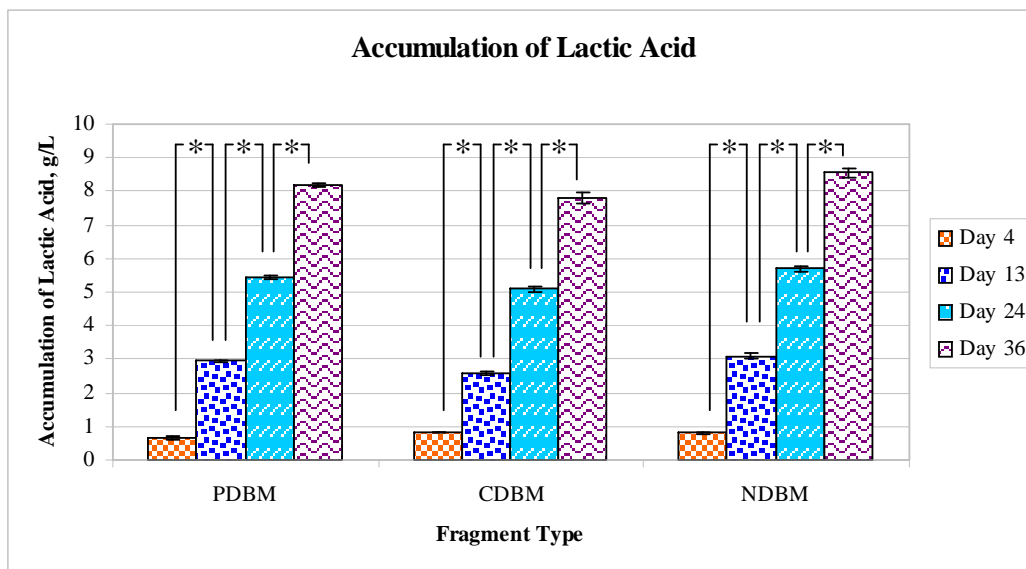


Figure 18 Lactic acid accumulation

Cumulative lactic acid production as a function of culture day. Each data point represents the mean of three values, and error bars denote the standard error of the mean (SEM).

Asterisks denote statistical differences ($p < 0.05$) in lactic acid levels with respect to time.

The cumulative consumption of glucose increased over time with respect to each fragment type . The total consumption of glucose increased significantly ($p < 0.05$) with time for each fragment type. The accumulation for each fragment type at each time point is displayed in Figure 19.

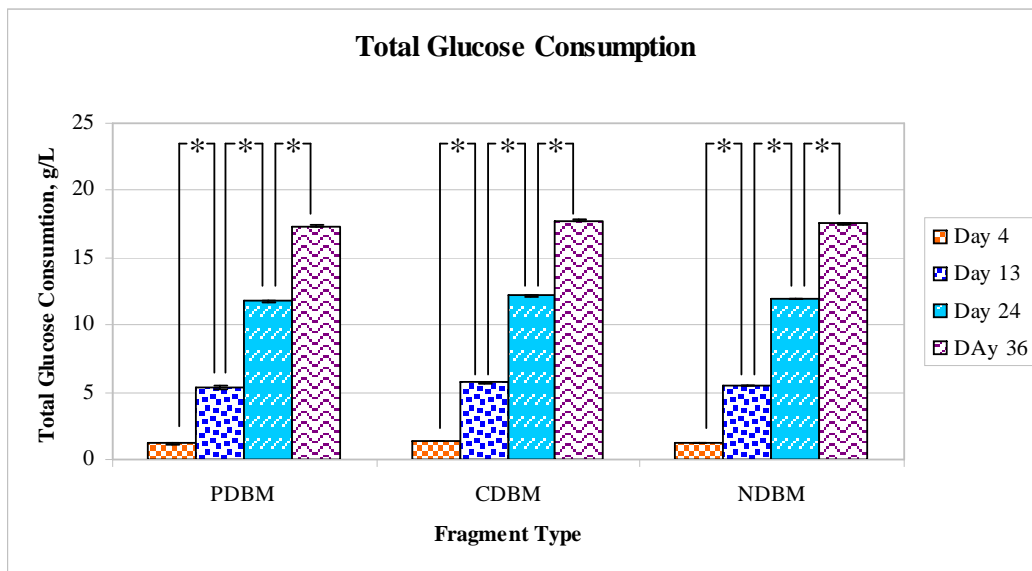


Figure 19 Cumulative glucose consumption
 Cumulative glucose consumption as a function of culture day. Each data point represents the mean of three values, and error bars denote SEM. Asterisks denote statistical differences ($p < 0.05$) in lactic acid levels with respect to time.

Alamar Blue[™]

The determination of metabolic activity of the D1 cells seeded on bone fragments indicates that, as time progressed, the cellular metabolic activity for each fragment type

increased significantly ($p < 0.05$) at varying times (Figure 20). Cells on all three fragment types, PDBM, CDBM, and NDBM, demonstrated a decrease in metabolic activity between Days 4 and 13, subsequently followed by an increase between Days 13 and 24. The measured metabolic activity of the cells loaded on the CDBM and NDBM fragments continued to increase between Days 24 and 36 while the cells seeded on PDBM fragments demonstrated a decrease in metabolic activity between these two time points. The metabolic activity of the cells on the PDBM fragments changed significantly ($p < 0.05$) between Day 4 and Day 13, Day 13 and Day 24, and in between Day 24 and Day 36. Metabolic activity of cells on the CDBM fragments changed significantly ($p < 0.05$) between Day 4 and Day 36 as well as between Day 13 and Day 24.

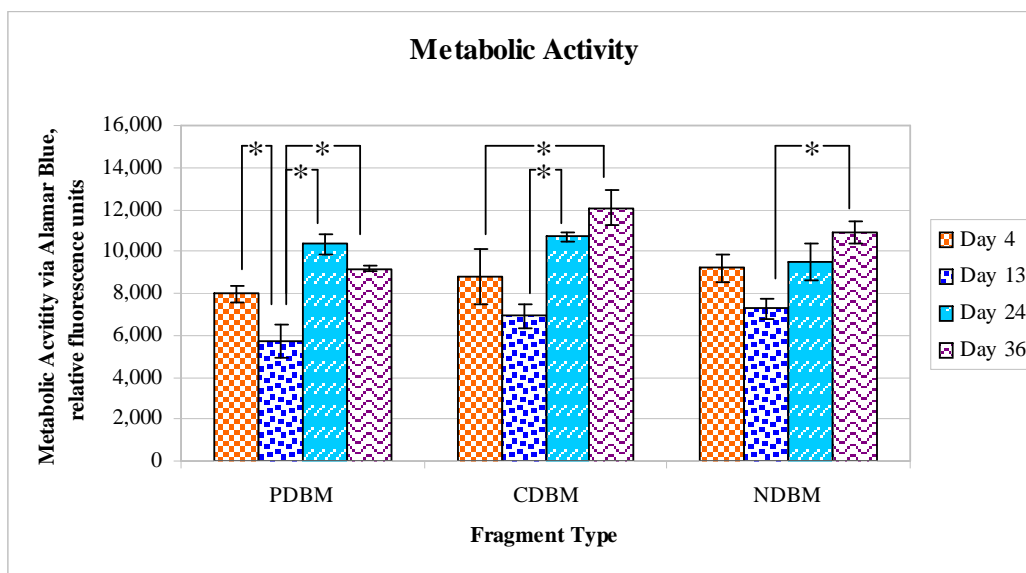


Figure 20 Metabolic activity via Alamar Blue™
 Metabolic activity as a function of culture day for each fragment type. Each data point represents the mean of three values, and error bars denote SEM. Asterisks denote statistical differences ($p < 0.05$) in lactic acid levels with respect to time.

Post-Study Quantitative Testing

Intracellular Protein

The intracellular protein level of D1 cells increased over time when seeded on PDBM, CDBM, and NDBM fragments (Figure 21). PDBM and CDBM cultures exhibited significant increases ($p < 0.05$) in protein level between Day 4 and Day 13 and again between Day 24 and Day 36. Although the protein levels in the PDBM and CDBM conditions decrease between Days 13 and 24, it was not a significant decrease ($p > 0.05$).

The NDBM condition showed a significant increase in protein level between Day 4 and Day 36 and between Day 13 and Day 36.

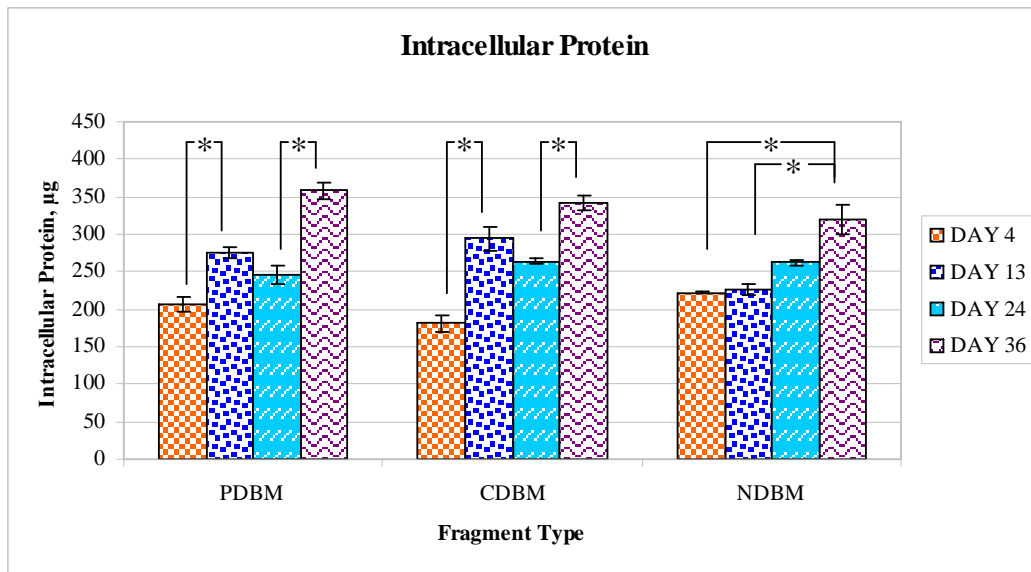


Figure 21 Intracellular protein

Intracellular protein level as a function each fragment type over time. Each data point represents the mean of three values, and error bars denote SEM. Asterisks denote statistical differences ($p < 0.05$) in lactic acid levels with respect to time.

Alkaline Phosphatase

The ALP activity level of PDBM increased over the course of the study (Figure 22). A significant increase ($p < 0.05$) occurred in ALP activity of cells seeded on PDBM fragments between Day 13 and Day 36. No significant ALP activity level differences ($p > 0.05$) were noted for the cellular CDBM and NDBM cultures (Figure 22).

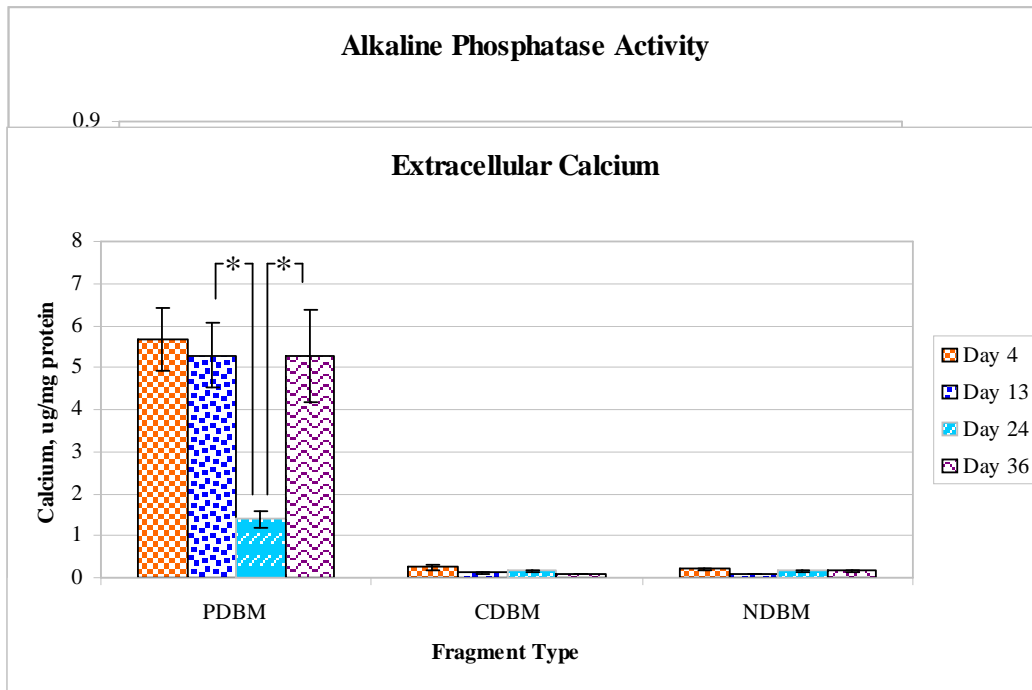


Figure 22 Alkaline phosphatase activity

ALP levels as a function of each fragment type over time. Each data point represents the mean of three values, and error bars denote SEM. Asterisks denote statistical differences ($p < 0.05$) in lactic acid levels with respect to time.

Extracellular Calcium

A significant decrease ($p < 0.05$) was found when comparing the level of extracellular calcium from PDBM samples from Day 13 and those from Day 24; a significant increase ($p < 0.05$) was noted when comparing samples from Day 24 and Day 36 (Figure 23). Larger levels of extracellular calcium were measured in PDBM than in cultures CDBM and NDBM cultures.

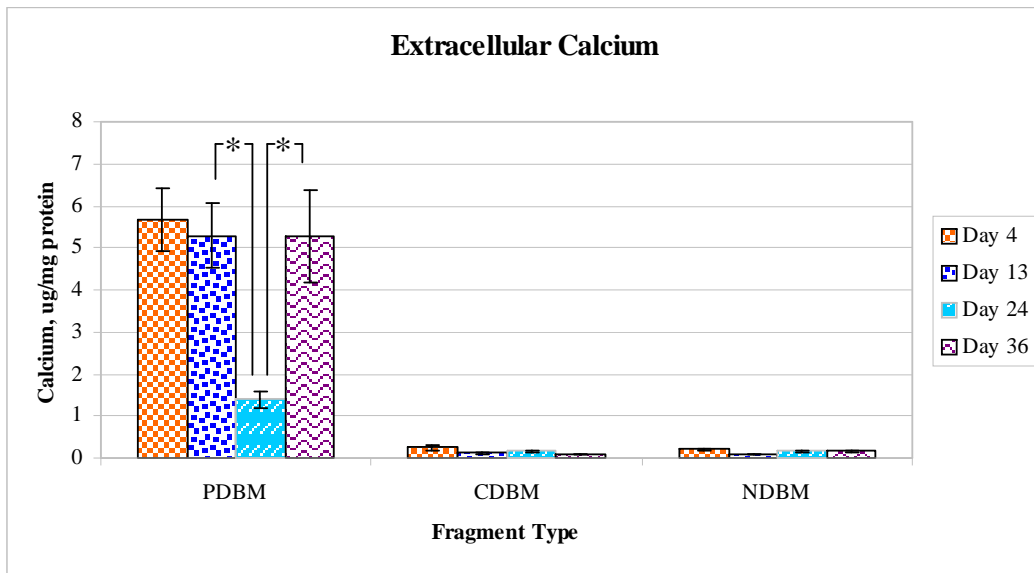


Figure 23 Extracellular calcium

Extracellular calcium levels as a function of each fragment type over time. Each data point represents the mean of three values, and error bars denote SEM. Asterisks denote statistical differences ($p < 0.05$) in lactic acid levels with respect to time.

Gene Expression

Real-Time RT-PCR

RNA concentrations, rRNA ratios, and integrity values obtained from the bioanalyzer are displayed in Table 9. Data displayed in Table 10 shows the number of reactions that occurred with respect to time for each gene studied. A maximum of three reactions were possible since three replicates were run for each fragment/time point combination. All Day 4 PDBM fragments demonstrated reactions at approximately the same cycle number. This is also true for Day 36 PDBM samples. Runx2 was not

expressed in Day 24 samples but BSP and OCN was expressed in all replicates for Day 24 PDBM samples. The number of CDBM replicates expressing Runx2, BSP, and OCN increased with time from Day 4 to Day 24. CDBM Day 36 cellular cultures demonstrated a decline in the number of replicates expressing BSP and OCN reactions, while three continued to express Runx2. Two Day 4 NDBM culture replicates expressed Runx2 and OCN, while replicate cultures from the remaining conditions and time points all had reactions indicative of Runx2 and OCN presence.

Table 9 Bioanalyzer results

Bioanalyzer results showing the RNA concentration and integrity of RNA samples

Note: N/A (not applicable) values result from undetectable values

Fragment Type	Time point	RNA concentration (ng/ μ L)	rRNA ratio (28s/18s)	RNA Integrity
PDBM	4	45	2.0	10.0
PDBM	4	22	2.2	10.0
PDBM	4	34	2.4	N/A
CDBM	4	43	2.0	10.0
CDBM	4	29	2.0	10.0
CDBM	4	27	2.1	N/A
NDBM	4	23	0.0	2.5
NDBM	4	34	2.6	10.0
NDBM	4	59	2.6	N/A
PDBM	13	81	2.3	10.0
PDBM	13	47	2.4	10.0
PDBM	13	50	2.5	9.9
CDBM	13	88	2.2	N/A
CDBM	13	84	2.2	N/A
CDBM	13	26	0.0	N/A
NDBM	13	57	2.5	N/A
NDBM	13	60	2.4	N/A
NDBM	13	58	2.4	N/A
PDBM	24	42	2.4	N/A
PDBM	24	48	2.4	N/A
PDBM	24	18	2.3	9.6
CDBM	24	37	2.3	N/A
CDBM	24	27	2.2	9.8
CDBM	24	26	2.4	10.0
NDBM	24	23	0.0	2.6
NDBM	24	35	2.3	10.0
NDBM	24	23	0.0	2.6
PDBM	36	41	2.0	10.0
PDBM	36	31	2.0	10.0
PDBM	36	15	1.9	9.5
CDBM	36	22	2.2	9.5
CDBM	36	27	1.9	9.8
CDBM	36	14	0.0	9.7
NDBM	36	26	2.4	N/A
NDBM	36	23	2.3	9.7
NDBM	36	21	1.6	N/A

Table 10 Real-time RT-PCR

Number of real-time RT-PCR reactions that occurred for each gene for each fragment type. The maximum number of reactions is three, since three replicates were run for each fragment condition at each time point.

Fragment Type	Day	RUNX	BSP	OCN
PDBM	4	3	3	3
PDBM	24	0	3	3
PDBM	36	3	3	3
CDBM	4	1	2	2
CDBM	24	3	3	3
CDBM	36	3	2	2
NDBM	4	2	3	2
NDBM	24	3	3	3
NDBM	36	3	3	3

DISCUSSION

Evaluation of Media Cocktails

The first stage of this research was to determine if osteogenic media supplements, specifically β -glycerophosphate and L-ascorbic acid, affect the cellular activity of D1 cells seeded on partially demineralized bone matrix when they are added to the media cocktail. The results of this study guided the media designation for the studies involving D1 cells and DBM.

Stereomicroscope images of DBM fragments prepared for the media study demonstrate that the particles have varying size, shape, and thickness, even though all the fragments were prepared in the same manner (Figure 4). The stereoscope images also show that the bone fragments demineralized at varying rates. After 80 minutes of demineralization, many fragments were partially demineralized; some were slightly demineralized; while others were either completely or almost completely demineralized. Images obtained after von Kossa staining on Day 4 (Figure 7) also demonstrate the variability in the mineralization levels of the bone fragments. It is likely that the variability in the demineralization rates occurred because of the initial variability in the size, shape, and thickness of the bone fragments.

Microscopic analysis of the substrates during the media cocktail study show that the cells adhered to the bottom of the well plate, while images obtained from cytotoxicity assays show that the cells also adhered to the surfaces of the bone. The wells of the 24-well plates were coated with Sigmacote™ prior to cell seeding. Sigmacote™ was designed to create a hydrophobic film with a neutral pH, that prevents proteins from adhering to

glass surfaces [56]. Although Sigmacote™ has been shown to efficiently coat select plastic surfaces, this product is not guaranteed to efficiently coat all film on plastic surfaces [56]. The cellular attachment on the well bottoms suggests that the coating process was not completely effective. As a result, the number of cells that initially attached to the bone surface likely differed between wells and also within each well. This situation could cause skewed results if, for example, a large difference was noted in the attachment levels on the substrates.

A significant difference in the total lactic acid production on Day 24 between the two media conditions indicates that PDBM substrates cultured in media containing osteogenic supplements were in a more acidic environment than those contained in the media without osteogenic supplements. Medium acidity can affect the cellular activity of cells in the medium. Below an extracellular pH of 7.1, osteoblast differentiation can be hindered [13]. The medium was slightly orange on later days of the study, indicating that the medium was not at an ideal pH. The medium should remain at a pH of 7.0-7.4 due to sodium bicarbonate in the initial medium solution. A color change indicates that the medium was either below a pH of 7.0 or nearing the outer bounds of the pH range indicated for α -MEM [13].

Histological and cell viability images indicate that D1 cells attached to the PDBM and CDBM substrates by Day 4. While some areas of the bone fragments appeared to increase in cellular number throughout the first study on both fragment types, other areas appeared to decrease. This decrease in cell number could be correlated to an increase in cell numbers that were rapidly proliferating on the surface of the wells. Between Days 13

and 24, the cells that were attached to the OSTEO AND NOSTEO system (PDBM fragments cultured with and without osteogenic supplements) well bottoms began to detach from the surface. The lower pH may have caused the detachment of cells from the substrates and wells, resulting in the lower number of cells visible on the surface OSTEO and NOSSTEO substrates on Day 24.

Relative comparisons of metabolic activity on 3D substrates can vary with cell cycle and cell number. For instance, a population of cells in the synthesis phase of cell growth spend their energy duplicating into daughter cells via DNA replication. Conversely, cells in the G_0 (resting) stage of interphase are not dividing and may be characterized by a different metabolic activity level than cells in the synthesis phase. Cells that are reacting negatively to a substrate may exhibit a spike in metabolic activity. Thus, the drop in metabolic activity level between Days 4 and 13 on the OSTEO (PDBM cultured with osteogenic supplemented media) and NOSTEO (PDBM cultured without osteogenic supplements) cultures could indicate that more cells were in the resting phase on Day 13 than on Day 4. The increase in metabolic activity level from Day 13 to Day 24 for OSTEO and NOSTEO cultures could mean that fewer cells were in the resting stage on Day 24 than at the previous time point. The metabolic activity assay, however, only yields a very general idea of the activity of the cells over 24 days. A more accurate picture might be obtained if the metabolic activity level was observed more often, perhaps at each medium change.

Figure 12 shows that, as time increased, the level of ALP also increased for all conditions. ALP, an active enzyme expressed in the plasma membrane of osteoblasts, is

an indirect indicator of the osteoinductivity of the DBM [13, 14]. It has been suggested that a direct correlation exists between the amount of ALP activity and the amount of new bone generation as induced by the scaffold [57]. ALP is required by the extracellular matrix for mineralization to occur within the scaffold [13, 57]. The increase in extracellular calcium in the samples cultured in medium containing osteogenic supplements suggests that mineralization of the samples is occurring.

Higher levels of protein were detected on the cellular control samples than on any of the other samples on Day 4 and Day 13. The control samples also had higher ALP levels on Day 13 and Day 24 than either experimental PDBM sample set. GnHCl treatment has been shown previously to be effective in removing osteoinductive proteins from substrates [58]. GnHCl extracts the BMPs from the substrate, resulting in inability of the substrate to induce bone formation [5]. The control substrates are osteoconductive, as evidenced by the cell attachment viewed through histological and live/dead images. These results suggest that the medium has a greater influence than the substrate on the proliferation and differentiation of the D1 cells.

No significant differences ($p > 0.05$) were detected between the two medium conditions on any particular time point with regard to the intracellular protein content, ALP activity, and extracellular calcium levels. The results of the assays performed on lactic acid and glucose levels, metabolic activity, and intracellular protein levels suggest that D1 cells proliferated on OSTEO (PDBM fragments cultured with osteogenic supplements) and NOSTEO (PDBM fragments cultured without osteogenic supplements) substrates [13]. Although significant differences existed between the metabolic activities

of the two experimental groups, no significant differences due to medium specification were evident with regard to proliferation and differentiation of D1 cells seeded on PDBM scaffolds.

Past research has shown that bone marrow stromal cells extracted from mice, and cultured in medium containing β -glycerophosphate and ascorbic acid, formed cells with polygonal morphology [59]. The polygonal cells from Falla's study stained positively following von Kossa staining, indicating that mineralization occurred [59]. In the same study, when one of these two media supplements was not added to the medium cocktail, mineralization did not occur [59]. Dexamethasone (Dex), a glucocorticoid, is often added to media as an osteogenic supplement since research has shown that the addition of this glucocorticoid leads to an increase in osteoblast marker expression in cell cultures with primary rat calvaria and primary rat marrow cells [13, 60, 61]. Although still used in medium cocktails when bone formation is a desired outcome, dexamethasone has been shown to inhibit bone formation in primary mouse marrow stromal cells [59].

In Vitro Evaluation of DBM

The second stage of this research was to evaluate the effects of the demineralization level on cellular activity over time. The cellular activity of cells seeded on completely demineralized bone fragments was compared to the cellular activity of cells seeded on partially demineralized bone fragments.

An alternative method of bone preparation was employed for the final evaluation of DBM. Stereomicroscope images taken before and during demineralization demonstrated that the bone fragments were more similar in physical structure when a rotor speed mill was used to grind the larger bone fragments into small pieces than when they were prepared for the media cocktail study. Images of fragments after 80 minutes of demineralization showed that the majority of the fragments had demineralization levels similar to each other (Figure 14). Although there were a few outliers which either demineralized quicker or slower than other fragments, the majority of the bone fragments had mineralized cores consistent with one another. Demineralization appeared to have occurred at a more consistent rate (Figure 14) than in previous demineralization attempts. Von Kossa images of the bone fragments at Day 4 (Figure 17) also support the theory that the PDBM fragments used in this study had consistent demineralization levels. CDBM fragments also showed complete demineralization in images obtained from stereomicroscopy and after von Kossa staining. Some of the CDBM fragments had small flecks of mineralized areas. Although stereomicroscope images made it appear that the fragments were completely demineralized, the fragments may have been able to undergo another demineralization cycle; however, care was taken to avoid excess demineralization of the bone fragments. Previous research has revealed that excessive demineralization decreases the osteoinductive properties of the substrate [5].

Due to the inconsistency with the Sigmacote™ well treatments, ultra-low attachment well plates were used for the final study. Microscopy of the cells and substrates throughout the study revealed that the cells did not adhere to the bottom of the

wells. LIVE/DEAD image analysis confirmed the lack of cells on the surface of the wells and the presence of cells covering the surface of the substrates (Figure 15). A direct comparison of the difference in the attachment of D1 cells on the bone fragments can be made from PDBM samples cultured in osteogenic supplemented media from the media cocktail study and PDBM samples in the final study. PDBM samples from the second study were more evenly demineralized than OSTEO fragments from the first study. On average, the PDBM samples had smaller demineralized cores than OSTEO fragments. On Day 4, a larger number of cells were detected on the PDBM samples than on the OSTEO samples. These fragments were cultured in the same media and both contained partially demineralized bone fragments. The ultra-low attachment plates and the consistency in fragment processing and demineralization likely improved the environment for cell attachment. It is also possible that the surfaces of the bone fragments differed between the two bone preparation methods. Cells might have been able to attach to the PDBM samples more readily than OSTEO samples.

All sets of bone fragments were metabolically active throughout the course of the study, as noted by the increase in lactic acid production and glucose uptake (Figure 18-19). Again, significant differences in metabolic activity via Alamar Blue™ (Figure 20) might demonstrate changes in cell cycle. The data from the lactic acid analysis, the glucose analysis, and the metabolic activity analysis show that the D1 cells were metabolically active on the PDBM, CDBM, and NDBM substrates.

As time progressed, the thickness of the cell layers attached to the outside of the bone fragments increased between each subsequent time point, as indicated by the H&E

images (Figure 16). By the end of the study, the PDBM fragments had more cell layers on the surface of the bone fragments than CDBM fragments and it appears that there was greater cellular infiltration of the PDBM fragments as compared to infiltration of the CDBM fragments.

It appears, based on the von Kossa images, that the cells on the PDBM fragments were causing mineralization (Figure 17). Images of the early time point specimens show the lining of the mineralized bone core with smooth edges; on the 24th day this edge, separating the mineralized and demineralized areas, was uneven and there were small specks of mineralized bone just outside the mineralized core. Day 36 von Kossa images show a very uneven line between the mineralized and demineralized areas of the bone. It is difficult to decipher if the cells on the CDBM fragments caused mineralization by the end of the study; since some of the fragments were not completely demineralized. It is not known whether or not the mineralized areas on Day 36 are a result of the fragments not being completely demineralized or a result of cellular mineralization.

Similar trends, showing a significant increase ($p < 0.05$) in intracellular protein between Days 4 and 13 and a drop in level between Days 13 and 24, followed by another significant ($p < 0.05$) increase between Days 24 and 36, occurred on both the PDBM and CDBM samples. These trends indicate that proliferation of D1 cells on the substrates occurred at approximately the same time points. An improved view of the differences in cellular response to the two fragments might be determined if the assay is run more frequently. Overall, there was an increase in proliferation over the course of the study.

ALP levels appeared to be consistent for the CDBM samples. A significant increase in cellular ALP levels was observed between Days 13 and 36 on the PDBM fragments. A combination of an increase in ALP activity and higher cell numbers within the PDBM fragments suggests that the oxygen and nutrients were adequate for cell growth and differentiation [62]. An increase in ALP activity was not noted for the CDBM fragments but an increase in cellular infiltration (H&E images) was noted over time. This behavior might indicate that differentiation was inhibited by the media conditions, such as the low pH.

The increase in cellular attachment and infiltration of the cells indicates that cellular proliferation did occur. It is possible that the PDBM fragments released BMPs at a more ideal rate than did the CDBM fragments, allowing osteoblast formation [38]. Chondrocytes and osteoblasts express ALP [63]. The presence of ALP activity suggests that the culture system can induce bone formation, although this point is not guaranteed.

An *in vitro* study by Zhang showed that over a range of residual calcium content percentages, 32.7%-1.2%, ALP activity level increased as the residual calcium level decreased from 32.7% to 2%. A subsequent decrease in ALP activity level was observed as the residual calcium level continued to decrease from 2% to 1.2% [5]. The lower ALP activity levels by cells seeded on CDBM substrates, as compared to PDBM substrates, indicates that the *in vitro* data obtained from this study correlate with Zhang's data. If the lower ALP values were not observed for the CDBM cultures it would not mean that the study contradicted previous work since the residual calcium levels before culture were not measured; therefore, the placement of the ALP activity levels on a bell curve (as

demonstrated by Zhang's data) is unknown. A review of clinical cases involving surface decalcified bone states that it is easier to contour the surface decalcified implants for the defect site [64]. It is not known what the surface decalcified implant is compared.

An *in vitro* study, reported in 2005 [33], evaluated the ALP activity of partially demineralized and fully demineralized substrates on Days 7 and 14 and resulted in similar ALP activity patterns as observed in the current study. ALP activity levels did not change drastically over time for the fully demineralized substrates, but increased for the partially demineralized substrates. It has been suggested that the difference in activity between PDBM and CDBM substrates could be that, as demineralization continues, osteogenic factors are removed, or that hydroxyapatite nucleation sites are exhausted [33]. The osteogenic factors that are exposed during demineralization are thought to recruit MSCs, which facilitate the bone induction principle [33, 36].

The consistent level of extracellular calcium in the NDBM and CDBM samples demonstrates that the cells in these samples were not mineralizing. The low and consistent levels of calcium could be a result of some of the fragments not being completely demineralized before seeding with cells and resulting in the release of calcium during the assay process. The PDBM samples had varying levels of calcium over the four time points studied. It is possible that human error caused the variation in results for the decrease in extracellular calcium. Perhaps when the lysates were removed from the wells for this assay they were not mixed properly causing the contents to be evenly distributed which would cause a skew in the results. This study did not include determining the extracellular calcium levels of fully mineralized bone fragments. If the

extracellular calcium level of fully mineralized bone fragments was known, then a comparison could be made concerning the amount of mineralization occurring over time for each of the sample groups.

RNA samples were inadvertently thawed for an unknown amount of time while they were in the -80°C freezer. RNA samples from Days 4, 13, and 24 were rerun on the Bioanalyzer once this problem was observed and it was determined from comparison of the results that Day 13 samples were not suitable for analysis since they were almost completely denatured (Table 22). When real-time RT-PCR was run, the data was acquired during the annealing stage. Therefore, it is inaccurate to run quantitative analysis on this data. It is feasible to determine if reactions occurred for each RNA sample. Table 23 shows that reactions occurred for all samples on all time points for all genes studied except for Runx2 on Day 24 for the PDBM samples. Mature genes such as osteocalcin were present in the CDBM and PDBM cultures. Other assays, such as von Kossa staining, completed on CDBM fragments did not show signs of mineralization. If signs of mineralization were evident, mature genes would be expected. The relative levels of gene expression are unknown so it is possible that the genes are expressed in low levels from CDBM samples and higher levels in PDBM samples, since mineralization appeared to occur in PDBM samples. Also, the presence of genes from real-time RT-PCR does not automatically mean that protein translation occurred *in vitro*, just that it has the possibility to occur. Real-time RT-PCR is measuring the protein translation from the reaction of the RNA with the primers and not the protein translation that occurred *in vitro*. Real-time RT-PCR should be repeated and data gathered during

the extension phases to give a better idea of the osteoblast activity over the course of the study since the RNA is being amplified during these stages.

The results presented in this thesis demonstrate that a difference in cellular activity was noted between PDBM and CDBM samples. These differences appear to be at which time points the cells were proliferating and differentiating. Thorough research on more time intervals should be completed to see these differences more accurately. This research appears to corroborate findings from other studies involving the differences between bone fragments of varying demineralization methods. Although it is also difficult to compare extracellular calcium levels, ALP activity levels, intracellular protein levels, and metabolic activity levels between this study and studies performed by other researchers due to discrepancies between preparation of samples and the specific equipment used, it is possible to note when and if cells are proliferating and differentiating.

CONCLUSIONS

Qualitative microscopy and quantitative assays indicate that D1 mouse stromal cells attach to PDBM substrates and subsequently proliferate and differentiate, regardless of whether the samples are cultured in medium containing osteogenic supplements. Contrary to prior results in the literature, the substrates cultured in medium containing osteogenic supplements did not differentiate faster than cells in the medium, without osteogenic supplements. Although the intent of the medium study was to examine partially demineralized substrates, visual analysis showed that the level of the substrate demineralization was minimal and variable. This variability likely caused skewed results.

Qualitative and quantitative assays also indicated that D1 cells attach to, proliferate, and differentiate on PDBM and CDBM scaffolds. The metabolic activity of the cells on the two scaffolds appeared to be similar. The proliferation and differentiation levels of D1 cells on the PDBM and CDBM scaffolds were significantly different on Day 24 of the study. According to von Kossa images and the varying levels of extracellular calcium extracted from the PDBM scaffolds, mineralization of the PDBM occurred between Day 24 and Day 36. Although the cells proliferated and differentiated on CDBM fragments, the assays performed showed no evidence of mineralization. The reactions that occurred from real-time RT-PCR demonstrate that cells were differentiating towards the osteoblast phenotype.

RECOMMENDATIONS

Further evaluation of the DBM scaffolds and preparation of the scaffolds is needed to fully evaluate the effectiveness of the scaffolds and the differences in bone formation triggered by PDBM versus CDBM samples. Additional studies should be performed to determine if the addition of dexamethasone to the media cocktail has inhibitory effects on bone formation.

Media conditions were acidic before each media change; decreasing the DBM/media proportion might allow a more physiological pH and higher rate of cellular proliferation and/or differentiation.

Further evaluation of the cellular activity of the cells needs to be completed in order to gain a better overall understanding of the cellular activity of the cells over time. All assays should be completed on Day 0 samples to offer a better comparison between later time points and the initial seeding of cells on the scaffold. Metabolic activity, intracellular protein, ALP, and extracellular calcium assays should be performed more often to gain a better overall understanding of the activity of the cells seeded on the substrates. Real time RT-PCR should be repeated in order to elucidate which genes are being expressed over time and to obtain a better understanding of osteoblast maturation in this system.

Previous studies examining the DBM substrates showed that the control culture, NDBM, had cellular activity similar to that found in PDBM and CDBM cultures. The activity of cells cultured on 2D surfaces in varying media conditions should be

investigated to determine if the proliferation and differentiation of D1 cells into osteoblasts can result from the media alone.

Studies should be performed to determine if the size of the bone particles might affect the ability of the cells to proliferate and differentiate. If a specific size fragment allows for greater cell to bone surface area then it is possible that this specific fragment size might be optimal for differentiation of the cells into osteoblasts.

In order to more completely evaluate the effectiveness of the proposed DBM preparation methods and the assays in an *in vitro* setting, *in vivo* studies should be conducted to assess the effects of DBM in a critical sized defect. This step will necessitate refining the DBM processing variables so that all fragments are of equal size, shape, thickness, and mineralization level. The *in vitro* characterization should be compared to the *in vivo* characterization to determine the efficacy of the *in vitro* model. *In vivo* models that demonstrate the effectiveness of DBM when care is taken in the processing of the scaffold might help companies and bone banks understand the importance of standardizing the preparation methods of DBM products. Once an accurate *in vitro* model is established, it would be interesting to evaluate the effects of non-steroidal anti-inflammatory drugs (NSAIDs) on the ability of the DBM scaffold to induce bone formation, since patients might receive these drugs as they are recovering from surgery or during the course of their recovery.

APPENDICES

Appendix A

H&E Staining Protocol

1. Rehydrate sections
 - a. 100% ETOH 10 dips
 - b. 100% ETOH 1 min
 - c. 95% ETOH 10 dips
 - d. 95% ETOH 1 min
2. Rinse in running tap water until “sheeting” action occurs
3. Soak in distilled water for one minute
4. Stain with hematoxylin for 5 minutes.
5. Rinse in running tap water until clear
6. Perform 12 dips in clarifier
7. Rinse in running tap water until “sheeting” action occurs
8. Soak in bluing reagent for one minute
9. Rinse in running tap water for one minute
10. Perform 10 dips in 95% ETOH
11. Stain with eosin for 45 seconds
12. Rinse in 2 changes of 95% ethanol. Perform 10 dips in each.
13. Rinse in 2 changes of 100% ethanol. Perform 10 dips in each.
14. Soak in 100% ethanol for one minute
15. Perform 10 dips in xylene followed by a 5 minute soak
16. Mount with paramount.

* This protocol was slightly modified from RICHARD-ALLAN™ HEMATOXYLIN & EOSIN protocol

Appendix B

Von Kossa Staining Protocol for GMA

1. Rehydrate sections.
 - a. Soak in 100% Ethanol for 2 minutes.
 - b. Soak in 95% Ethanol for 2 minutes.
 - c. Soak in distilled Water for 2 minutes.
2. Stain with 2% silver nitrate for 30 minutes in sunlight or UV light.
3. Rinse slides thoroughly with distilled water until water is clear.
4. Stain with hematoxylin for 6 minutes.
5. Rinse slides thoroughly with distilled water until water is clear.
6. Rinse with 0.25% ammonium hydroxide for 10 seconds.
7. Rinse slides thoroughly with distilled water until water is clear.
8. Stain with 0.3% eosin Y for 5 minutes.
9. Rinse slides thoroughly with distilled water until water is clear.
10. Rinse with 2 changes of 95% Ethanol. Perform 15 dips in each.
11. Rinse with 2 changes of 100% Ethanol. Perform 15 dips in each.
12. Soak in xylene. Perform 10 dips followed by a 1 minutes soak.
13. Soak in xylene for 5 minutes.
14. Mount with paramount.

* Protocol was obtained from Dr. Chuck Thomas (dissertation) and slightly modified.

Appendix C

Primer Design Protocol

1. On the National Center for Biotechnology Information's (NCBI) webpage, www.ncbi.nlm.nih.gov/, search for the gene(s) of interest.
2. Locate appropriate gene and follow the link to the mRNA sequence on the GenBank data page.
3. Highlight and paste the sequence into the nucleotide/nucleotide BLAST search at www.ncbi.nlm.nih.gov/BLAST. Choose a homologous mRNA sequence that contains a "complete CDS" sequence
4. Paste the mRNA CDS sequence into the mRNA sequence box in Spidey found at www.ncbi.nlm.nih.gov/IEB/Research/Ostell/Spidey/
5. Paste the original genomic sequence from step 1 into the genomic sequence box on the Spidey webpage.
6. Align the genomic and mRNA sequences in Spidey.
7. Open the Primer 3 homepage, frodo.wi.mit.edu/cgi-bin/primer3/primer3_www.cgi. Paste in the mRNA derived complete cds from the NCBI page
 - a. The search parameters should be set as follows:
 - i. Human mis-priming library
 - ii. Create a new sequence ID for the primer
 - iii. Product size range: 100-150
 - iv. Number of results to return: 10
 - v. Primer Size: 18/20/22
 - vi. Melting Temperature: 60/62/65
 - vii. GC%: 40/50/60
 - viii. Mex self-complimentary: 5
 - ix. Max 3' complimentarity: 2
 - x. Max Poly-X: 3
 - xi. GC clamp: 1
 - b. Search for primers
8. From the Primer 3 output, choose a primer that is close to the 3' end, binds to portions of at least 2 different exons (ideally with >400 basepairs intervening the genomic sequence).
9. Validate primer choice by copy and pasting the forward primer into BLAST, typing in at least 10 intervening bases. Copy and paste in the reverse primer immediately following the intervening base pairs. Perform BLAST search.
10. Verify that the expected products match the targeted gene.
11. Order primers from Integrated DNA Technologies (IDT) using the primer sequences from Primer 3 for each targeted gene.

* This protocol was obtained from class notes presented by Dr. Ken Webb for a Bioengineering Cell Analysis Class

LITERATURE CITED

1. Bostrom, M.P.G. and D.A. Seigerman, *The Clinical Use of Allografts, Demineralized Bone Matrices, Synthetic Bone Graft Substitutes and Osteoinductive Growth Factors: A Survey Study*. HSSJ, 2005. **1**(1): p. 9-18.
2. Giannoudis, P.V., H. Dinopoulos, and E. Tsiridis, *Bone substitutes: an update*. Injury, 2005. **36 Suppl 3**: p. S20-7.
3. Greenwald, A.S., et al., *Bone-graft substitutes: facts, fictions, and applications*. J Bone Joint Surg Am, 2001. **83-A Suppl 2 Pt 2**: p. 98-103.
4. Hing, K.A., *Bone repair in the twenty-first century: biology, chemistry or engineering?* Philos Transact A Math Phys Eng Sci, 2004. **362**(1825): p. 2821-50.
5. Zhang, M., R.M. Powers, Jr., and L. Wolfenbarger, Jr., *Effect(s) of the demineralization process on the osteoinductivity of demineralized bone matrix*. J Periodontol, 1997. **68**(11): p. 1085-92.
6. Dwyer, D.P. and M.D. Cohen (2003) *Musculoskeletal Manifestations of Chronic Kidney Disease*. Bulletin on the Rheumatic Diseases.
7. Pilitsis, J.G., D.R. Lucas, and S.S. Rengachary, *Bone healing and spinal fusion*. Neurosurg Focus, 2002. **13**(6): p. e1.
8. Manolagas, S.C., *Birth and death of bone cells: basic regulatory mechanisms and implications for the pathogenesis and treatment of osteoporosis*. Endocr Rev, 2000. **21**(2): p. 115-37.
9. Groeneveld, M.C., V. Everts, and W. Beertsen, *Alkaline phosphatase activity in the periodontal ligament and gingiva of the rat molar: its relation to cementum formation*. J Dent Res, 1995. **74**(7): p. 1374-81.
10. Becker, W., B.E. Becker, and R. Caffesse, *A comparison of demineralized freeze-dried bone and autologous bone to induce bone formation in human extraction sockets*. J Periodontol, 1994. **65**(12): p. 1128-33.

11. Mastrogiacomo, M., et al., *Tissue engineering of bone: search for a better scaffold*. Orthod Craniofac Res, 2005. **8**(4): p. 277-84.
12. Vaccaro, A.R., *The role of the osteoconductive scaffold in synthetic bone graft*. Orthopedics, 2002. **25**(5 Suppl): p. s571-8.
13. Thomas, C.B., *Development of a Composite Bone Graft Substitute for Bone Tissue Engineering Applications*, in *Bioengineering*. 2005, Clemson University: Clemson. p. 274.
14. Gitelis, S. and P. Saiz, *What's new in orthopaedic surgery*. J Am Coll Surg, 2002. **194**(6): p. 788-91.
15. Grauer, J.N., et al., *Bone graft alternatives for spinal fusion*. BioDrugs, 2003. **17**(6): p. 391-4.
16. Vilquin, J.T. and P. Rosset, *Mesenchymal stem cells in bone and cartilage repair: current status*. Regen Med, 2006. **1**(4): p. 589-604.
17. Ishaug, S.L., et al., *Bone formation by three-dimensional stromal osteoblast culture in biodegradable polymer scaffolds*. J Biomed Mater Res, 1997. **36**(1): p. 17-28.
18. Gurevitch, O., et al., *Reconstruction of cartilage, bone, and hematopoietic microenvironment with demineralized bone matrix and bone marrow cells*. Stem Cells, 2003. **21**(5): p. 588-97.
19. Liu, Y., et al., *Accelerated Repair of Cortical Bone Defects Using a Synthetic Extracellular Matrix to Deliver Human Demineralized Bone Matrix*. Journal of Orthopaedic Research, 2005: p. 1454-1462.
20. Porter, B.D., et al., *Mechanical properties of a biodegradable bone regeneration scaffold*. J Biomech Eng, 2000. **122**(3): p. 286-8.

21. Russell, J.L. and J.E. Block, *Clinical utility of demineralized bone matrix for osseous defects, arthrodesis, and reconstruction: impact of processing techniques and study methodology*. Orthopedics, 1999. **22**(5): p. 524-31; quiz 532-3.
22. Takikawa, S., et al., *Comparative evaluation of the osteoinductivity of two formulations of human demineralized bone matrix*. J Biomed Mater Res A, 2003. **65**(1): p. 37-42.
23. Peter, S.J., et al., *Marrow stromal osteoblast function on a poly(propylene fumarate)/beta-tricalcium phosphate biodegradable orthopaedic composite*. Biomaterials, 2000. **21**(12): p. 1207-13.
24. Hallfeldt, K.K., et al., *Sterilization of partially demineralized bone matrix: the effects of different sterilization techniques on osteogenetic properties*. J Surg Res, 1995. **59**(5): p. 614-20.
25. Langer, R. and J.P. Vacanti, *Tissue engineering*. Science, 1993. **260**(5110): p. 920-6.
26. University, B.T.E.C.a.C.M., *Bone Tissue Engineering*.
27. Case, E.D., I.O. Smith, and M.J. Baumann, *Microcracking and porosity in calcium phosphates and the implications for bone tissue engineering*. Mat Sci Eng A, 2004. **390**: p. 246-254.
28. Logeart-Avramoglou, D., et al., *Engineering bone: challenges and obstacles*. J Cell Mol Med, 2005. **9**(1): p. 72-84.
29. Chen, Q.Z., I.D. Thompson, and A.R. Boccaccini, *45S5 Bioglass-derived glass-ceramic scaffolds for bone tissue engineering*. Biomaterials, 2006. **27**(11): p. 2414-25.
30. Jones, J.R., L.M. Ehrenfried, and L.L. Hench, *Optimising bioactive glass scaffolds for bone tissue engineering*. Biomaterials, 2006. **27**(7): p. 964-73.

31. Walsh, W.R. and D.L. Christiansen, *Demineralized bone matrix as a template for mineral-organic composites*. Biomaterials, 1995. **16**(18): p. 1363-71.
32. Mardas, N., et al., *Denaturation of demineralized bone matrix significantly reduces bone formation by guided tissue regeneration*. Clin Oral Implants Res, 2003. **14**(6): p. 804-11.
33. Mauney, J.R., et al., *In vitro and in vivo evaluation of differentially demineralized cancellous bone scaffolds combined with human bone marrow stromal cells for tissue engineering*. Biomaterials, 2005. **26**(16): p. 3173-85.
34. Altundal, H., H. Sayrak, and C. Delilbasi, *Effect of Demineralized Bone Matrix on Resorption of Autogenous Cortical Bone Graft in Rats*. Turk J Med Sci, 2005. **35**: p. 209-216.
35. Chesmel, K.D., et al., *Healing response to various forms of human demineralized bone matrix in athymic rat cranial defects*. J Oral Maxillofac Surg, 1998. **56**(7): p. 857-63; discussion 864-5.
36. Urist, M.R., et al., *The bone induction principle*. Clin Orthop Relat Res, 1967. **53**: p. 243-83.
37. Dubuc, F.L.a.U., M.R., *The Accessibility of the Bone Induction Principle in Surface-Decalcified Bone Implants* Clinical Orthopaedics and related research, 1967. **55**: p. 217-223.
38. Shih, H.N., et al., *Restoration of bone defect and enhancement of bone ingrowth using partially demineralized bone matrix and marrow stromal cells*. J Orthop Res, 2005. **23**(6): p. 1293-9.
39. Harakas, N.K., *Demineralized bone-matrix-induced osteogenesis*. Clin Orthop Relat Res, 1984(188): p. 239-51.
40. Murugan, R. and S. Ramakrishna, *Modification of demineralized bone matrix by a chemical route*. The Royal Society of Chemistry, 2004. **14**: p. 2041-2045.

41. Ranly, D.M., et al., *Platelet-derived growth factor inhibits demineralized bone matrix-induced intramuscular cartilage and bone formation. A study of immunocompromised mice.* J Bone Joint Surg Am, 2005. **87**(9): p. 2052-64.
42. Finkemeier, C.G., *Bone-grafting and bone-graft substitutes.* J Bone Joint Surg Am, 2002. **84-A**(3): p. 454-64.
43. Urist, M.R., *Surface-decalcified allogeneic bone (SDAB) implants. A preliminary report of 10 cases and 25 comparable operations with undecalcified lyophilized bone implants.* Clin Orthop Relat Res, 1968. **56**: p. 37-50.
44. Urist, M.R. and B.S. Strates, *Bone formation in implants of partially and wholly demineralized bone matrix. Including observations on acetone-fixed intra and extracellular proteins.* Clin Orthop Relat Res, 1970. **71**: p. 271-8.
45. Zhang, M., R.M. Powers, Jr., and L. Wolfinbarger, Jr., *A quantitative assessment of osteoinductivity of human demineralized bone matrix.* J Periodontol, 1997. **68**(11): p. 1076-84.
46. Groeneveld, E.H., et al., *Mineralization processes in demineralized bone matrix grafts in human maxillary sinus floor elevations.* J Biomed Mater Res, 1999. **48**(4): p. 393-402.
47. Lomas, R.J., et al., *An evaluation of the capacity of differently prepared demineralised bone matrices (DBM) and toxic residuals of ethylene oxide (EtOx) to provoke an inflammatory response in vitro.* Biomaterials, 2001. **22**(9): p. 913-21.
48. Han, B., B. Tang, and M.E. Nimni, *Quantitative and sensitive in vitro assay for osteoinductive activity of demineralized bone matrix.* J Orthop Res, 2003. **21**(4): p. 648-54.
49. Herold, R.W., et al., *The effects of varying degrees of allograft decalcification on cultured porcine osteoclast cells.* J Periodontol, 2002. **73**(2): p. 213-9.
50. Schwartz, Z., et al., *Ability of commercial demineralized freeze-dried bone allograft to induce new bone formation.* J Periodontol, 1996. **67**(9): p. 918-26.

51. Traianedes, K., et al., *Donor age and gender effects on osteoinductivity of demineralized bone matrix*. J Biomed Mater Res B Appl Biomater, 2004. **70**(1): p. 21-9.
52. Meinel, L., et al., *Bone tissue engineering using human mesenchymal stem cells: effects of scaffold material and medium flow*. Ann Biomed Eng, 2004. **32**(1): p. 112-22.
53. Delloye, C., A. Hebrant, and L. Coutelier, *The effects of a long-term preservation of the bone inductive capacity of hydrochloric acid (HCl)-decalcified matrix*. Clin Orthop Relat Res, 1986(205): p. 309-10.
54. Gilbert, L., et al., *Expression of the osteoblast differentiation factor RUNX2 (Cbfa1/AML3/Pebp2alpha A) is inhibited by tumor necrosis factor-alpha*. J Biol Chem, 2002. **277**(4): p. 2695-701.
55. Komori, T., *Requisite roles of Runx2 and Cbfb in skeletal development*. J Bone Miner Metab, 2003. **21**(4): p. 193-7.
56. Sigma, *Sigmacote Product Information*.
57. Cui, K., et al., *A Porous Scaffold from Bone-like Powder Loaded in a Collagen-Chitosan Matrix*. Journal of Bioactive and Compatible Polymers, 2004. **19**: p. 17-21.
58. Sampath, T.K. and A.H. Reddi, *Dissociative extraction and reconstitution of extracellular matrix components involved in local bone differentiation*. Proc Natl Acad Sci U S A, 1981. **78**(12): p. 7599-603.
59. Falla, N., et al., *Characterization of a 5-fluorouracil-enriched osteoprogenitor population of the murine bone marrow*. Blood, 1993. **82**(12): p. 3580-91.
60. Shin, H., et al., *Osteogenic differentiation of rat bone marrow stromal cells cultured on Arg-Gly-Asp modified hydrogels without dexamethasone and beta-glycerol phosphate*. Biomaterials, 2005. **26**(17): p. 3645-54.

61. Peter, S.J., et al., *Osteoblastic phenotype of rat marrow stromal cells cultured in the presence of dexamethasone, beta-glycerolphosphate, and L-ascorbic acid.* J Cell Biochem, 1998. **71**(1): p. 55-62.
62. Kasten, P., et al., *Comparison of human bone marrow stromal cells seeded on calcium-deficient hydroxyapatite, beta-tricalcium phosphate and demineralized bone matrix.* Biomaterials, 2003. **24**(15): p. 2593-603.
63. Harris, M.T., et al., *Mesenchymal stem cells used for rabbit tendon repair can form ectopic bone and express alkaline phosphatase activity in constructs.* Journal of Orthopaedic Research, 2004. **22**(5): p. 998-1003.
64. Osbon, D.B., et al., *Bone grafts with surface decalcified allogeneic and particulate autologous bone: report of cases.* J Oral Surg, 1977. **35**(4): p. 276-84.